Geoscience Frontiers 10 (2019) 2287–2300

HOSTED BY

Contents lists available at ScienceDirect

China University of Geosciences (Beijing)

Geoscience Frontiers

journal homepage: www.elsevier.com/locate/gsf

Research Paper

Early Cretaceous transpressional and transtensional tectonics straddling the Sulu orogenic belt, East China

Jun Wang [a,b], Su-Chin Chang [b], Yong Chen [c,*], Shiyong Yan [c]

[a] School of Resource Environment and Earth Sciences, Yunnan University, Kunming 650500, China
[b] Department of Earth Sciences, The University of Hong Kong, Hong Kong, China
[c] School of Geosciences, China University of Petroleum (East China), Qingdao 266580, China

ARTICLE INFO

Article history:
Received 3 October 2018
Received in revised form
17 January 2019
Accepted 2 April 2019
Available online 18 April 2019
Handling Editor: Christopher J Spencer

Keywords:
Detrital zircon
Seismic reflection
Structural analysis
Tectonic evolution
Early Cretaceous

ABSTRACT

The Sulu orogenic belt (SOB) separates the North and South China blocks in East Asia and formed during Triassic continent-continent collision. However, late Mesozoic post-collisional exhumation is poorly understood due to lack of surface evidence for Paleo-Pacific subduction and associated effects. This paper interprets the tectonic history of the SOB using detrital zircon age data from Early Cretaceous sedimentary units along with previously published geochronologic and geochemical data to reconstruct sedimentological and tectonic history. Detrital zircon age distributions obtained from sedimentary units include a 2.0 Ga subpopulation that appears only in turbidite units to the southeast. This sediment probably derived from the Yangtze Block. Terrestrial facies from the Jiao-Lai basin to the northwest appear to derive from the North China Block. Geochronologic and geochemical data indicate that Early Cretaceous, post-collisional volcanism was compositionally bimodal (mafic-felsic) with associated intrusive activity that peaked at 120 Ma. Seismic images of northerly regions of the study area indicate this occurred in an extensional setting. Sedimentary facies and field structural analyses revealed an unconformity interpreted to reflect rapid uplift with NW–SE compression to the south. Given observed sinistral movement along the Tan-Lu fault, we interpret northwest and southeast regions of the SOB as experiencing transtensional and transpressional tectonics, respectively, driven by continuous subduction of the Paleo-Pacific Plate. Intrusion of the Late Yanshannian granitoids marked the final formational stage of this unique tectonic setting.

1. Introduction

Large orogenic belts along continental margins typically form due to thickening and shortening caused by lithospheric collision. The Sulu orogenic belt (SOB) constitutes the eastern segment of the largest high pressure to ultra-high pressure metamorphic belt in the world (>4000 km, Fig. 1), the Kunlun-Qinling-Dabie-Su-Lu orogenic belt. The Kunlun-Qinling-Dabie-Su-Lu orogenic belt formed during Triassic collision of the North China (NCB) and the South China blocks (Zhao and Coe, 1987; Okay and Şengör, 1992; Yin and Nie, 1993; Li, 1994; Lin and Li, 1995). The SOB extends from the Jiangsu province in the north to the Shandong province of East China (Fig. 1) in the east, which represents the tectonic boundary between the NCB and the Yangtze Block (YZB, northern segment of the South China Block) (Yang, 2002).

Sedimentary assemblages of adjacent basins record post-collisional uplift and denudation history of the SOB (e.g. Li et al., 2012; Xie et al., 2012; Wang et al., 2016a). The Jiao-Lai basin (JLB) to the north formed due to sinistral strike-slip movement along the Tan-Lu fault (TLF) triggered by subduction of the Paleo-Pacific Plate beneath the NCB in the Early Cretaceous (Zhu et al., 2005, 2010; Sun et al., 2007). The geochemical character of widespread Early Cretaceous igneous rocks in east Shandong generally indicate an extensional setting related to tectonic collapse of lithosphere thickened by the NCB-South China bock collision (e.g. Guo et al., 2005; Yang et al., 2005; Ling et al., 2009; Ma et al., 2014; Tang et al., 2014; Wang et al., 2015). Cretaceous terrestrial sedimentary and volcaniclastic rocks indicate that the Cretaceous section of the JLB developed within an extensional setting (Lu and Dai, 1994; Sun et al., 2007; Zhang et al., 2008) along the TLF before a change in the

* Corresponding author.
E-mail address: yongchenzy@upc.edu.cn (Y. Chen).
Peer-review under responsibility of China University of Geosciences (Beijing).

https://doi.org/10.1016/j.gsf.2019.04.007

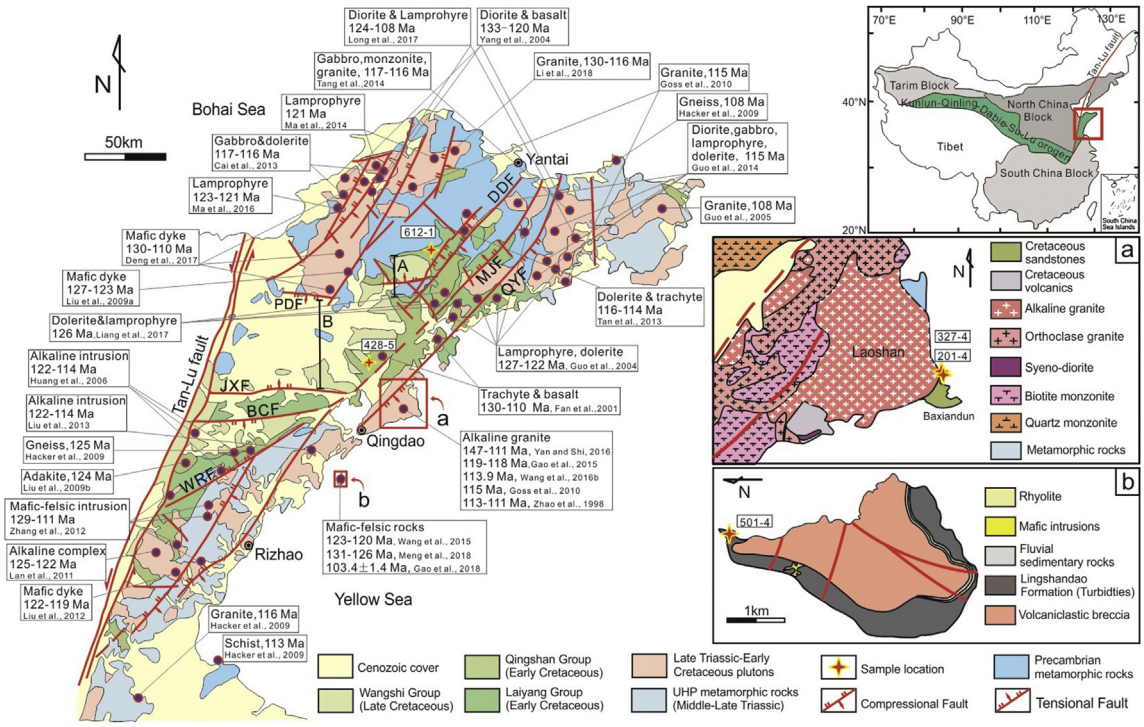

Fig. 1. Geological map of east Shandong, China (modified after Xie et al., 2012), with sampling locations and geochronologic constraints provided by Early Cretaceous magmatic events. (a) Enlarged geological map of Laoshan granites and Baxiandun (modified after Wang et al., 2016b) showing sample locations; (b) enlarged geological map of Lingshan Island (modified after Wang et al., 2014) with sample locations. Main faults: BCF—Baichihe Fault, PDF—Pingdu Fault, JXF—Jiaoxian Fault, WRF—Wulian-Rongcheng Fault, MJF— Muping-Jimo Fault, QYF — Qingdao-Yantai Fault, and DDF —Dongdoushan Fault. A and B are transects associated with the two seismic reflection profiles shown in Fig. 7. The ages for igneous rocks as marked in the left were cited from: Zhao and Coe (1987); Guo et al. (2004, 2014); Huang et al. (2006); Zheng and Zhang (2007); Hacker et al. (2009); Goss et al. (2010); Liu et al. (2012, 2013); Cai et al. (2013); Tan et al. (2013); Gao (2015); Ma et al. (2016); Yan and Shi (2016); Deng et al. (2017); Liang et al. (2017); Long et al. (2017); Li et al. (2018); Meng et al. (2018).

subduction direction of the Paleo-Pacific Plate from roughly southward to northwestward at ~125–122 Ma (Sun et al., 2007).

Studies addressing evidence of Triassic collision between the NCB and YZB (e.g. Zheng et al., 2003; Ernst et al., 2007; Liou et al., 2009) have not yet provided a consistent explanation for subsequent middle to late Mesozoic crust-mantle interaction and related magmatic events (e.g. Griffin et al., 1998; Menzies et al., 2007; Liu et al., 2009a, b). Meanwhile, the far field effects of Paleo-Pacific Plate movement on the Kunlun-Qinling-Dabie-Su-Lu orogenic belt (Zhu et al., 2005, 2010; Sun et al., 2007) and tectonic evolution of the SOB during the Early Cretaceous also remain poorly understood. Recent studies of turbidites deposited southeast of the SOB (e.g. Lu et al., 2011; Zhang et al., 2013; Wang et al., 2014) detected evidence of a sedimentary source area different from that which fed the JLB in the northwest (e.g. Xie et al., 2012). Wang et al. (2016b) also reported a tectonic shift in east Shandong from a transpressional to a transtensional setting. However, links between Paleo-Pacific Plate subduction and regional tectonic events such as the formation of the JLB, strike-slip movement along the TLF, SOB denudation history, and ongoing large-scale igneous activity in this area remain unclear. This contribution interprets detrital zircon data from Early Cretaceous sedimentary units around the SOB along with regional geochemical, geochronologic, and structural data in order to constrain understanding of the region's tectonic history.

2. Geological background

The SOB is situated in the southeastern part of east Shandong, north China, and is bound by the TLF in west Shandong (Fig. 1). Studies of the SOB describe an initial prograde metamorphic event at 247–244 Ma (Liu et al., 2006, 2007) followed by peak eclogite-facies metamorphism at 240–215 Ma (Yang et al., 2004; Liu et al., 2007; Zhao et al., 2007; Tang et al., 2008) and exhumation at 215–205 Ma (Chen et al., 2003; Wallis et al., 2005; Liu et al., 2007; Leech and Webb, 2013). The SOB includes ultrahigh pressure and high pressure metamorphic belts in the northwest and southeast, respectively (e.g. Ernst and Liou, 1995; Leech et al., 2006; Ratschbacher et al., 2006). To the northwest, the Baichihe-Qingdao-Yantai fault separates the SOB from the JLB while the Yellow Sea flanks the SOB to the southeast (Fig. 1). In terms of rock types, the SOB exposed in east Shandong divides into three general assemblages. The northeast and southwest assemblages consist primarily of gneisses and Yanshannian granitoid intrusions with minor Cretaceous terrestrial sedimentary rocks. Intervening exposures between these two assemblages consist primarily of Cretaceous terrestrial sedimentary rocks and granitoid intrusions (Fig. 1).

Two geological provinces lie generally north of the SOB. These include the JLB and the East Shandong Complex (ESC), located to the southwest and northeast of each other, respectively (Fig. 1). The JLB consists of (in ascending order from underlying Precambrian NCB basement) the Early Cretaceous lacustrine Laiyang Group, the volcaniclastic Qingshan Group, and the Late Cretaceous fluvial Wangshi Group. The ESC consists of Proterozoic meta-sedimentary sequences overlying the Archean Jiaodong terrane (Wu et al., 2014a, b). The former includes the Neoproterozoic Penglai Group overlying the Paleoproterozoic Fenzishan, Jingshan, and Zhifu groups (Zhou et al., 2004; Zhai et al., 2005; Tang et al., 2007). The latter consists primarily of granitoid gneisses with minor supracrustal rocks (Bai and Dai, 1998; Tang et al., 2007).

Mesozoic igneous units also occur on a widespread basis throughout the SOB in east Shandong (Fig. 1). These units include the Late Triassic Shidao alkaline complex emplaced along the

northeast edge of the SOB at ca. 225–201 Ma (Chen et al., 2003; Guo et al., 2005; Yang et al., 2005), Late Jurassic plutons emplaced in northeasterly areas of east Shandong at 161–142 Ma (Hu et al., 2004; Guo et al., 2005), and a series of NE–SW trending Early Cretaceous magmatic rocks emplaced at 143–111 Ma with the major crystallization event at 130–125 Ma (Zhao and Zheng, 2009 and references therein). The Late Triassic alkaline complex potentially formed from magmatism during exhumation and was caused by dehydration melting of ultrahigh pressure metamorphic material with affinities to the YZB (Zhao and Zheng, 2009). Geochemical signatures from Late Jurassic plutons are consistent with partial melting of the YZB continental crust at a depth of >40 km (Zhang et al., 2004; Guo et al., 2005) but researchers have yet to establish the geodynamic mechanism for these events. Westward subduction of the Paleo-Pacific Plate beneath the Eurasian plate likely caused the extensive Early Cretaceous magmatism observed throughout eastern China (Hacker et al., 1995; Ratschbacher et al., 2000; Zhu et al., 2005, 2010; Zhou et al., 2006).

Two early Mesozoic marine sedimentary formations have been recently recognized in the central SOB (e.g. Fu and Yu, 2010; Wu et al., 2010; Lu et al., 2011; Wang et al., 2014). The Lingshandao Formation (LSF) of Lingshan Island, southwest of Qingdao City, China, exhibits a depositional age of ca. 121 Ma (Wang et al., 2014). The Baxiandun Formation (BXF) occurs in easterly areas around Laoshan Mountain, east of Qingdao City, China. An earlier Late Ordovician age estimate for the unit (Fu and Yu, 2010; Wu et al., 2010) was recently revised to Early Cretaceous (121–120 Ma) by Wang et al. (2016b). The sedimentary environment represented by the BXF remains under debate. For example, Fu and Yu (2010) and Wu et al. (2010) interpreted the BXF as marine turbidites based on a weak, negative Ce/Ce* anomaly. Sun et al. (2014) also proposed a marine environment based on high Sr and Ba concentrations and Sr/Ba ratios approaching those observed from Cenozoic and modern marine sediments, relatively low Th/U and high V/(V + Ni) ratios, and a weak, negative Ce/Ce* anomaly. However, Wu and Fu (2014) reinterpreted their own data along with the weak Ce/Ce* anomaly reported by Fu and Yu (2010) and Wu et al. (2010) to indicate deep water lacustrine sedimentary conditions. Despite this interpretation, similar lithologies and detrital zircon age distributions for the LSF and BXF imply shared provenance and similar depositional ages for these two formations (Wang et al., 2014, 2016b). They likely represent the same basin.

A series of E–W and NE–SW faults occur around east Shandong. Faults bounding the JLB trend primarily in an E–W direction, while other faults around east Shandong generally trend NE–SW, a direction consistent with the dominant trends of the SOB and JLB boundaries (Zhang et al., 2006b). The Baichihe-Qingdao-Yantai fault and the TLF form the southern and western margins of the JLB (respectively). While mechanisms for the JLB's development remain cryptic (e.g. Lu and Dai, 1994; Dai et al., 1995; Xu, 2001; Wu et al., 2004; Zhang et al., 2006b; Li et al., 2012), most published research agrees that it formed in an intracontinental extensional setting.

3. Sampling strategy and analytical methods

To evaluate sedimentary provenance, determine differences among Early Cretaceous units along the SOB, and further constrain its tectonic evolution, we collected five Early Cretaceous sedimentary units throughout the central SOB and analyzed their detrital

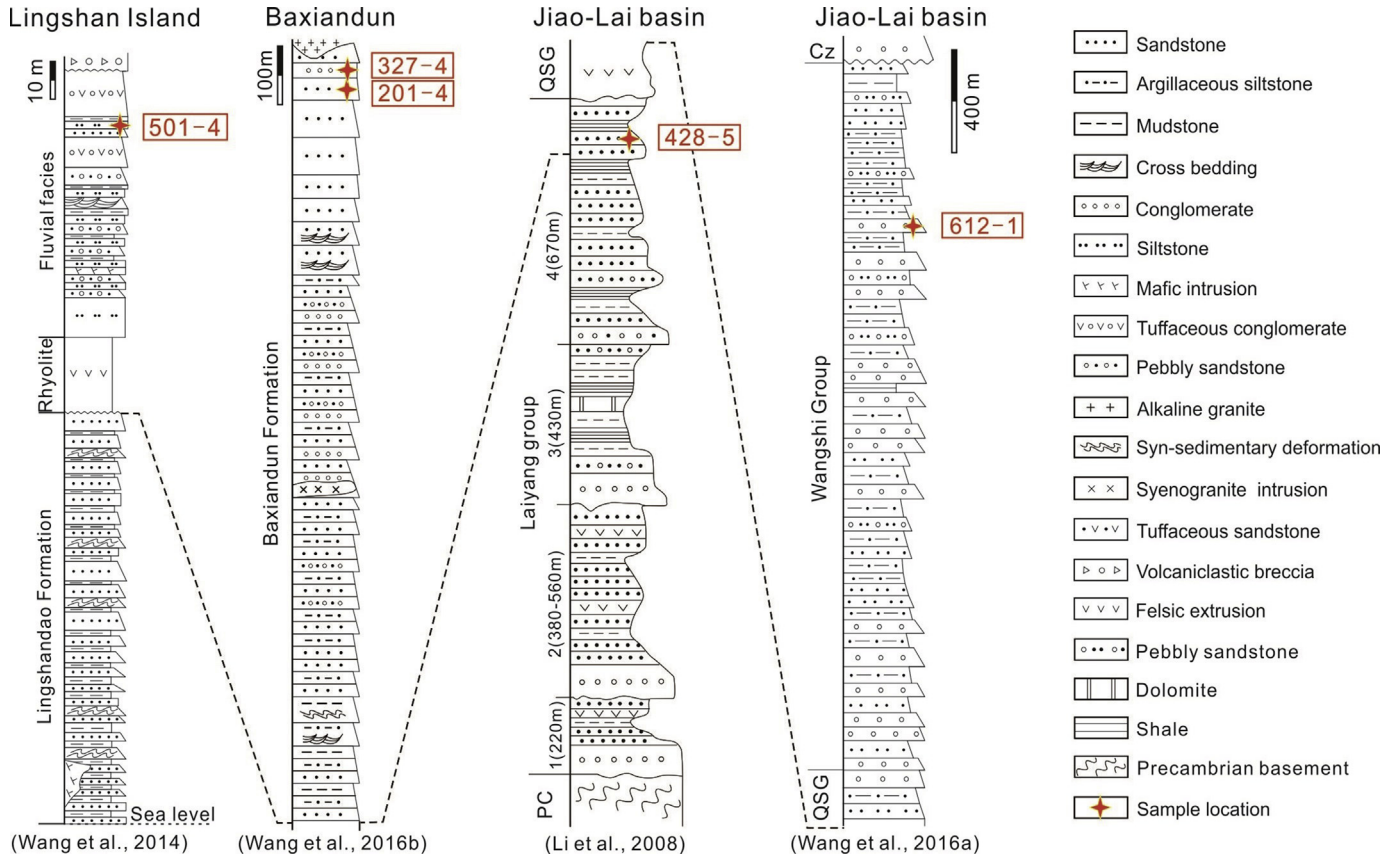

Fig. 2. Stratigraphic columns showing sample locations from four sections on Lingshan Island, at Baxiandun, and within the Jiao-Lai basin. QSG–Qingshan Group, PC–Precambrian basement, and Cz–Cenozoic. The angular unconformity between the LSF and its overlying rhyolite in the Lingshan Island are also shown in Fig. 8.

zircon age distributions (Figs. 1 and 2). These included a medium-grained sandstone (612-1) from the Wangshi Group (a unit that hosts dinosaur fossils) and a pebbly coarse-grained sandstone (428-5) from the Laiyang Group. Both of these deposited in the JLB (Appendix A1). We also collected a coarse-to medium-grained sandstone (501-4) from fluvial units exposed on Lingshan Island, a boulder-sized gneissic clast (327-4) from a conglomeratic unit, and a coarse-grained shore facies sandstone (201-4) from the BXF. Sampling locations are shown in Figs. 1 and 2, sample photos are shown in Fig. 3, and Appendix A1 lists zircon U–Pb data.

Detrital zircons were prepared for analysis at the Institute of Earth Science, Academia Sinica, Taiwan, China. Rock samples were crushed and sieved to isolate the 60–200 μm size-fraction. This size fraction was washed several times to remove fines and less dense components, then dried and separated with a magnetic separator. Zircons were hand-picked (selected randomly) under optical microscope and mounted in epoxy resin. Hardened mounts were sectioned and polished to expose the grains' midsections at about 2/3 of their width. We then imaged the zircon grains using a JSM-6360LV Electron Probe Microanalyzer equipped with a mini-cathodoluminescent (CL) detector system. Fig. 4 shows representative zircon CL images.

Detrital zircon U–Pb isotope data were obtained using a Multi Collector Inductively Coupled Plasma-Mass Spectrometer (MC-ICP-MS) equipped with a New Wave Research LUV213 laser ablation (LA) system, available through the Department of Earth Sciences at the University of Hong Kong. The LA system generates a 213 nm UV light beam using a frequency-quintupled Nd:YAG laser. Most analyses were performed with a 30 μm beam diameter, 6 Hz repetition rate and an energy of 0.6–1.3 mJ per pulse. Instrumental settings and procedural details follow those given in Xia et al. (2004) and Zheng et al. (2018). We used standard zircon 91500 (Wiedenbeck et al., 1995) as a primary calibration standard and GJ-1 as a secondary reference. Mounted detrital zircon grains were selected randomly for dating. U–Pb ages were calculated using the Isoplot/Ex 3.0 software (Ludwig, 2003). The Microsoft Excel macro developed by Andersen (2002) was used for common Pb correction. Appendix A1 lists all age analyses with 1σ errors and Fig. 5 plots age data on concordia diagrams with 1σ uncertainties calculated at the 95% confidence interval. Given a 15% discordance range for all the U–Pb ages, we interpreted $^{206}Pb/^{238}U$ ages for zircons younger than 1000 Ma and $^{207}Pb/^{206}Pb$ ages for older grains.

To build a comprehensive picture of sedimentary provenance and Early Cretaceous basins surrounding the SOB, more than 6000 zircon ages were compiled from previously published studies and plotted as probability density diagrams and histograms for comparison (Fig. 6, references in Appendix A2). Seismic images of the JLB document the Early Cretaceous extensional history of northerly areas of the SOB (Fig. 7). Seismic data were obtained and interpreted by the Institute of Petroleum Exploration & Development, Shengli Oil Field, Sinopec Group. Field observations and structural analyses (Figs. 8 and 9) of Early Cretaceous sedimentary rocks were performed around southerly regions of the SOB to help constrain tectonics and depositional history. Geochemical and geochronologic data from igneous rocks emplaced within the SOB during the interval of interest (Fig. 10) were also used to interpret tectonic setting.

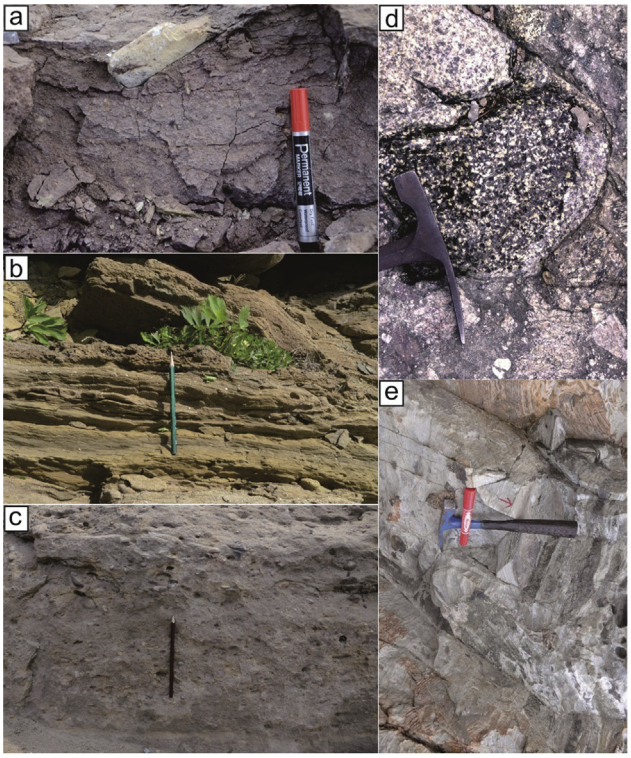

Fig. 3. Photos showing outcrop features for sample localities. (a) Medium-grained sandstone 612-1 from the Wangshi Group, a Jiao-Lai basin deposit that hosts dinosaur fossils, (b) coarse to medium-grained sandstone 501-4 from fluvial units occurring on Lingshan Island, (c) pebbly to coarse-grained sandstone 428-5 from the Laiyang Group in the Jiao-Lai basin, (d) gneissic boulder 327-4 from the Baxiandun Formation conglomerate, and (e) coarse-grained sandstone 201-4 from the Baxiandun Formation, interpreted as a shore facies depositional environment. Pencils were ~20 cm in length, the marker was ~15 cm in length, and the hammers were ~30 cm in length by 18 cm in width.

4. Results

Zircons from different samples and age populations differed in terms of their morphology and internal structure. As shown in Fig. 4, Early Cretaceous and Neoproterozoic zircons generally exhibited euhedral morphologies, oscillatory zoning patterns, and length/width ratios of 1.5–2. We interpreted these features as indicative of igneous origins. By contrast, Triassic, Paleoproterozoic, and Archean zircons show subrounded morphologies and light or dark, homogeneous, inherited cores with bright, narrow rims (<10 μm). We interpreted these features as indicating metamorphic origins, recrystallization, or significant transport and modification prior to final deposition.

We analyzed 100 zircon grains for sample 612-1 and 90 grains for the other four samples. Appendix A1 lists Th/U isotopic ratios, U–Pb isotopic ratios and calculated ages. Concordant U–Pb ages (discordance less than 15%) are plotted on concordia and probability density diagrams (Figs. 5 and 6, respectively). The grains with euhedral morphologies and oscillatory zoning patterns show higher Th/U ratios while grains with subrounded morphologies and homogeneous inherited cores show lower Th/U ratios.

Sixty-nine concordant ages were obtained for sandstone sample 612-1 from the Wangshi Group. The age distribution included four major subpopulations at 136–110 Ma, 796–588 Ma, 1.9–1.8 Ga, and 2.5–2.4 Ga, as well as a minor Triassic subpopulation and sporadic Paleozoic and Mesoproterozoic ages. Most of the Early Cretaceous and Neoproterozoic zircons exhibited relatively high Th/U ratios of 0.4–2.2, whereas Triassic, Paleoproterozoic, and Archean zircons gave Th/U ratios of <0.4.

Sandstone 428-5 from the Laiyang Group yielded 83 concordant ages with four major subpopulations at 132–126 Ma, 243–227 Ma, 831–718 Ma, and 1.9–1.8 Ga, as well as sporadic Paleozoic, Paleoproterozoic, and Archean ages. Most of the Triassic and 1.9–1.8 Ga zircons gave Th/U ratios of <0.4 whereas most of the Early

Fig. 4. CL images of typical detrital zircon grains analyzed in this study. The spot size of 30 μm corresponds to the laser beam diameter.

Cretaceous, Neoproterozoic, and Archean zircons gave Th/U ratios of 0.4–1.9.

Sandstone 501-4 from a Lingshan Island fluvial unit gave 78 concordant ages with two major subpopulations at 860–657 Ma and 2.5–2.0 Ga along with one Paleozoic age. Neoproterozoic zircons gave Th/U ratios of greater than 0.7 except in the case of one grain with Th/U = 0.1. Older zircons typically exhibited Th/U ratios of <0.7.

Sixty-six concordant ages from a boulder-sized clast in the BXF (327-4) gave mostly Neoproterozoic ages (831–568 Ma) along with solitary Cambrian (535 Ma) and Paleoproterozoic (2.0 Ga) ages. Th/U ratios for these zircons ranged of 0.5–2.1, whereas the sole Paleoproterozoic zircon gave Th/U ratio of 0.04.

Sandstone 201-4 from the BXF gave 76 concordant ages that included three major age populations at 865–648 Ma, 1.9–1.8 Ga, and 2.0 Ga, along with three minor age populations at 133–120 Ma, 239–217 Ma, and 2.3 Ga. The age distribution also included sporadic Early Cretaceous, Neoproterozoic, and Paleoproterozoic (2.0 Ga) ages associated with relatively high Th/U ratios of 0.5–2.0. Zircons forming the Paleoproterozoic subpopulation typically showed Th/U ratios of <0.5.

The seismic reflection profiles (Fig. 7) show a series of south-dipping and north-dipping listric normal faults running along respective northern and southern margins of the JLB. The faults cut through the youngest Wangshi Group (Late Cretaceous) and Precambrian basement, and the fault planes become flatter and converge along a deep, uniform detachment fault. Fault throws increase while sediment accumulation decreases with depth. These indicate Early Cretaceous development of listric features as growth faults in an extensional setting.

Conjugated joints appear on Lingshan Island to the south of the SOB. We obtained 20, 81, 30, and 16 groups of joint plane attitudes (data listed in Appendix A3) for the LSF as it occurs in four different sections on Lingshan Island (Fig. 9). Sterographic projection of these data reveals a roughly NW–SE compressive stress field. A "Z" shaped asymmetric fold was identified in the LSF, under the angular unconformity between the LSF and its overlying rhyolite (Fig. 8).

Fig. 10 compares major element geochemical data for 525 samples of the 140–100 Ma igneous rocks of the JLB gathered from previous studies (data and references listed in Appendices A4 and A5). Plots of total alkali-silica (TAS) and Na_2O vs. K_2O indicate

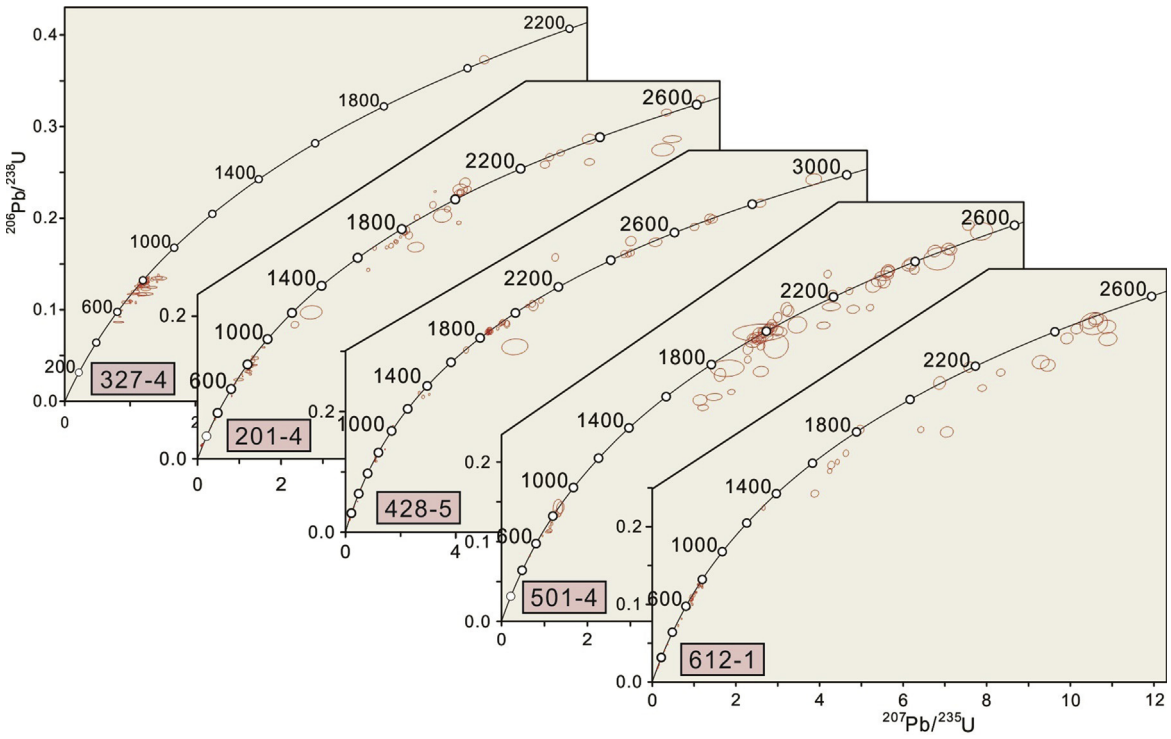

Fig. 5. Concordia diagrams of detrital zircon U–Pb ages for the samples analyzed in this study.

predominantly basaltic to basaltic-andesitic and rhyolitic compositions. We compiled 1563 zircon ages for these rocks and plotted them as probability density diagrams. These ages cluster at 130–110 Ma with a remarkable peak at ~120 Ma.

5. Discussion

5.1. Sedimentary provenance interpretations

The five samples (327-4, 201-4, 428-5, 501-4, and 612-1) analyzed for detrital zircon age populations included six major subpopulations. These consist of Early Cretaceous (136–110 Ma), Triassic (243–217 Ma), Neoproterozoic (865–568 Ma), Paleoproterozoic (2.0 Ga and 1.9–1.8 Ga), and Archean to Paleoproterozoic (2.5–2.3 Ga) age ranges as shown in Fig. 6.

The Early Cretaceous subpopulation included zircons which exhibited euhedral morphologies, oscillatory zoning patterns, and Th/U ratios typically >0.4 (Fig. 4 and Appendix A1). This subpopulation likely represents Early Cretaceous igneous rocks found throughout east Shandong (Zhao and Zheng, 2009). An Early Cretaceous cooling event caused by a rapid exhumation of the SOB, as proposed by Lin et al. (2005), may have also contributed these zircons to local basins.

Triassic zircons exhibiting low Th/U ratios (mostly ≤0.1), subrounded zircon morphologies, and inherited cores with overgrowth rims that indicate metamorphic or recycled origins probably derived from the SOB. These likely reflect a Triassic metamorphic event that occurred roughly around 247–205 Ma (e.g. Chen et al., 2003; Yang et al., 2003; Liu et al., 2004, 2006, 2007; Wallis et al., 2005; Leech and Webb, 2013) due to continent-continent collision between the YZB and the NCB (Okay and Şengor, 1992; Yin and Nie, 1993; Li, 1994; Lin and Li, 1995; Gilder et al., 1999).

Neoproterozoic zircon populations also generally exhibit oscillatory zoning patterns and euhedral morphologies indicative of magmatic origin. Neoproterozoic ages among inherited zircon cores from the ultrahigh pressure metamorphic rocks may derive from SOB protoliths that intruded Mesoproterozoic to Archean basement material of the YZB (Zheng et al., 2003; Liu and Liou, 2011). The presence of this subpopulation within Mesozoic basins of east Shandong was therefore used to distinguish sedimentary input from the NCB and YZB (Zheng et al., 2003; Xie et al., 2012; Wang et al., 2014). Neoproterozoic zircons thus indicate a sediment source area that included SOB protoliths found in the YZB.

Archean to Paleoproterozoic ages detected in the samples analyzed here included subpopulations at 2.5–2.3 Ga, 2.0 Ga, and 1.9–1.8 Ga. These ages likely reflect contribution from adjacent tectonic blocks, the NCB, YZB, and SOB. Previous large-scale studies conducted on the NCB have documented several magmatic and metamorphic events occurring from 2.9 Ga to 2.2 Ga, including an early crust-forming episode at ~2.9–2.7 Ga (Zhai and Liu, 2001; Zhai et al., 2005), a remarkable high-grade metamorphic event at 2.6–2.45 Ga (Zhai and Liu, 2001; Zhai et al., 2005; Zhao et al., 2005; Tang et al., 2007; Zhao, 2014), two emplacement events at 2.2–2.1 Ga (Li and Zhao, 2007), and a high pressure metamorphic event at 1.95–1.8 Ga (e.g. Zhao et al., 2000, 2002; Zhai and Liu, 2003; Tam et al., 2011, 2012; Wu et al., 2014a, b). By contrast, the YZB experienced Precambrian crystallization events at 1.2–1.0 Ga and 850–700 Ma (e.g. Li et al., 2003a, b; Zheng and Zhang, 2007; Zheng et al., 2008a, b). A significant YZB tectonothermal event at ca. 2.0 Ga has been interpreted as playing an essential role in the craton's middle Paleoproterozoic tectonic evolution (e.g. Zhang et al., 2006a; Liu et al., 2008; Zhao and Zheng, 2009). This even occurred slightly, notably earlier than a 1.95–1.8 Ga event in the NCB to the north of the SOB, as indicated in Fig. 6 (East Shandong Complex and the JLB). Even though the 2.0 Ga zircons have been detected in Paleoproterozoic sedimentary facies of the Liaohe Group in the Eastern Block of the NCB (Li and Zhao, 2007), these have only been detected in southern Liaoning and not in the JLB (Xie et al., 2012; Wang et al., 2016a; Fig. 6). We therefore interpret the Paleoproterozoic age population at 2.0 Ga as unique evidence

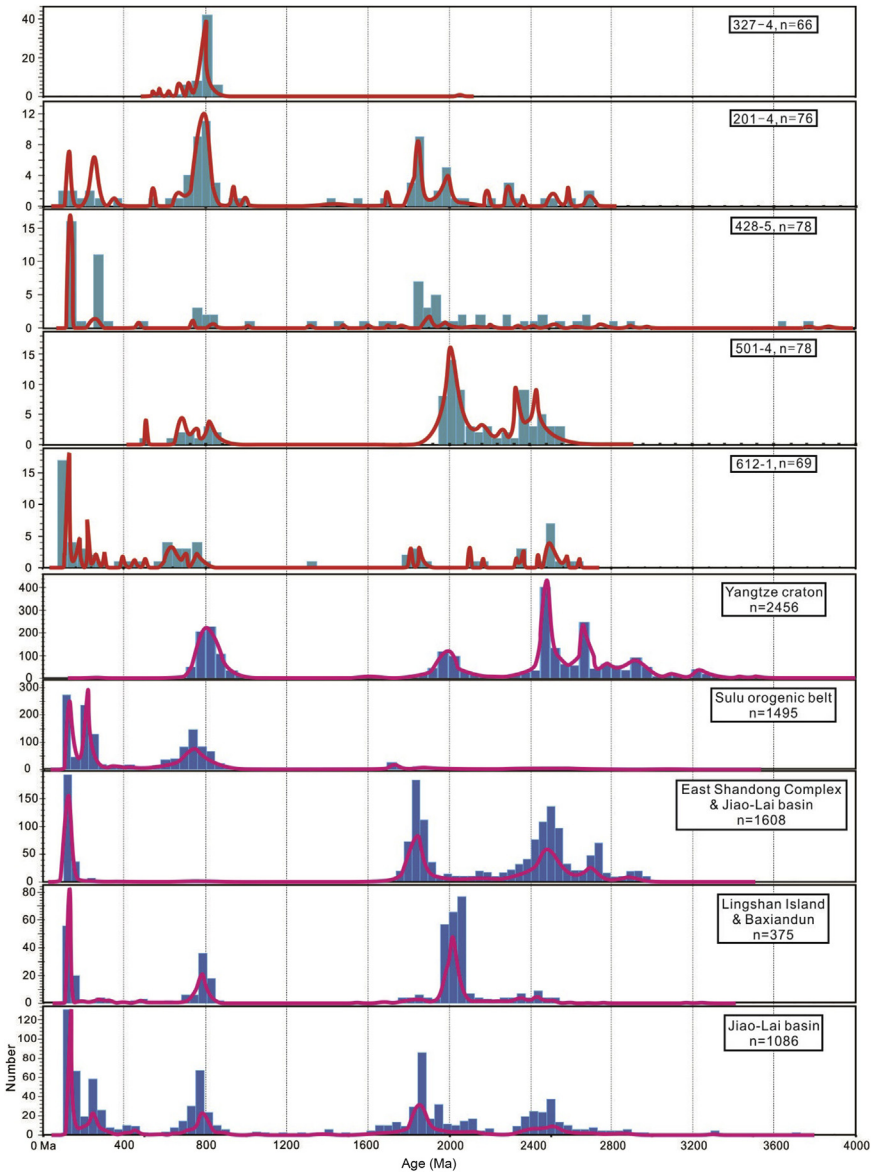

Fig. 6. Cumulative probability plots and frequency histograms of detrital zircon U–Pb age populations measured in this study (upper five diagrams) compared with potential provenance around the Sulu Orogenic belt (lower five diagrams). Age data for the lower five diagrams were compiled from published references listed in Appendix A2.

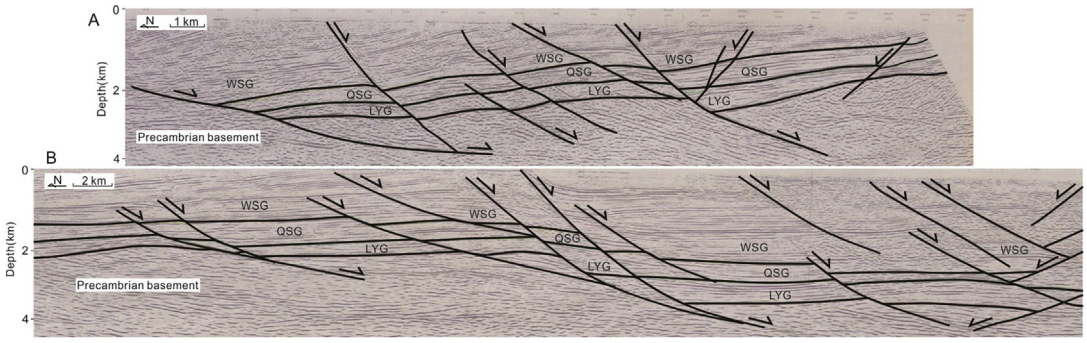

Fig. 7. Two seismic reflection profiles for the central Jiao-Lai basin (marked in Fig. 1), to the NW of the SOB. LYG–Early Cretaceous Laiyang Group, QSG–Early Cretaceous Qingshan Group, and WSG–Late Cretaceous Wangshi Group.

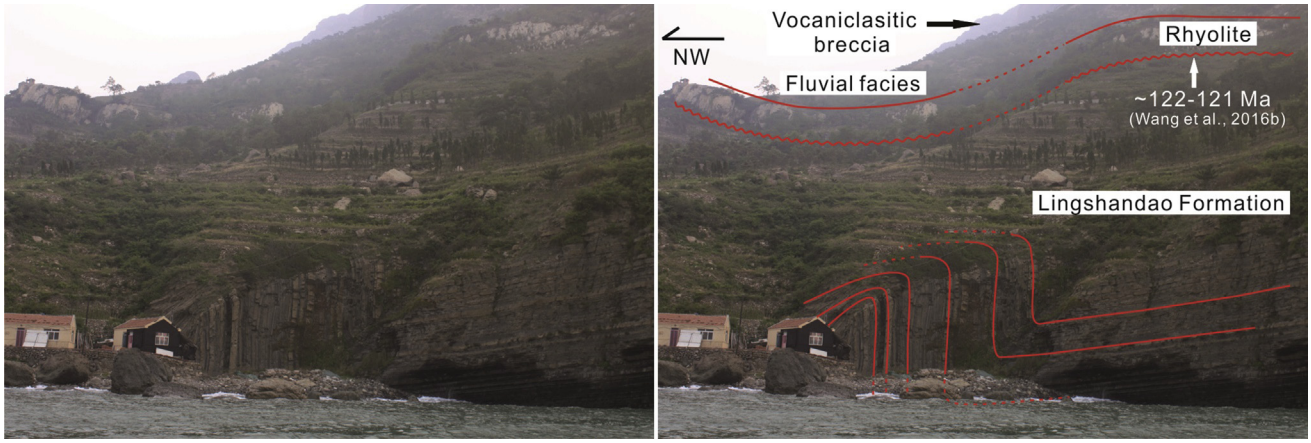

Fig. 8. Field photographs with simplified structure depiction showing the fold below the unconformity on Lingshan Island southeast of the SOB indicating a NW–SE compressional regime at ~122–121 Ma. The angular unconformity between the LSF and its overlying rhyolite is also marked in Fig. 2.

for a sedimentary contribution from the YZB. Lu et al. (2011) identified a series of syn-sedimentary slump structures in the LSF, including slump folds with NE–SW hinge line directions and NW axial plane dip directions, both of which support the interpretation of source material transported from the southeast, where the YZB is located. The 2.0 Ga age feature also appears in cumulative probability plots and histograms (Fig. 6) of U–Pb age data compiled from previous studies. Fig. 6 shows an additional Archean subpopulation at 3.0–2.7 Ga. This age feature further disqualifies the NCB as a source area (e.g. Zhou et al., 2008a, b).

5.2. Sedimentary units surrounding the SOB show different provenance signatures

Both the LSF and BXF, and the JLB, from which provenance samples were collected and analyzed, represent basins adjacent to the SOB (Fig. 1). Detrital age distributions of samples collected from each basin differ markedly from one another. To rigorously examine provenance differences between these two basins, we compared the data presented here with detrital zircon U–Pb age data published in previous studies (Fig. 6).

Sample 327-4 (gneissic boulder) from the BXF generally exhibits only one Neoproterozoic age subpopulation with fairly high Th/U ratios (0.5–2.1). The oscillatory zoning patterns and absence of growth rims or other signs of metamorphic alteration from the Triassic NCB and YZB collision generally indicate magmatic origins for zircons from this sample. Together, this sample's similarity with a majority of other clasts in the conglomerate along with its stratigraphic position near the top of the BXF, which indicates a shore facies depositional environment, suggest that nearby Neoproterozoic protoliths in the SOB, originally from the YZB, represent the source material for this subpopulation (Fig. 6).

The age distributions of sandstones 501-4 and 201-4 from the basin to the southeast of the SOB share two major Neoproterozoic and Paleoproterozoic (2.0 Ga) subpopulations. Sample 501-4 exhibits only three subpopulations and lacks ages younger than Neoproterozoic, suggesting the SOB, YZB, and ESC as source areas. This age distribution resembles that observed for sandstone samples collected from Lingshan Island (Wang et al., 2014) indicating a similar or shared source area. By contrast, the age distribution from sample 201-4 indicates multiple sources consistent with Early Cretaceous igneous material found throughout east Shandong, the ESC, SOB, and YZB. Age distributions from both sandstone samples include a distinctive 2.0 Ga subpopulation, which coincides with a significant tectonothermal event affecting the YZB (Zhang et al., 2006a; Liu et al., 2008). Our results therefore support the

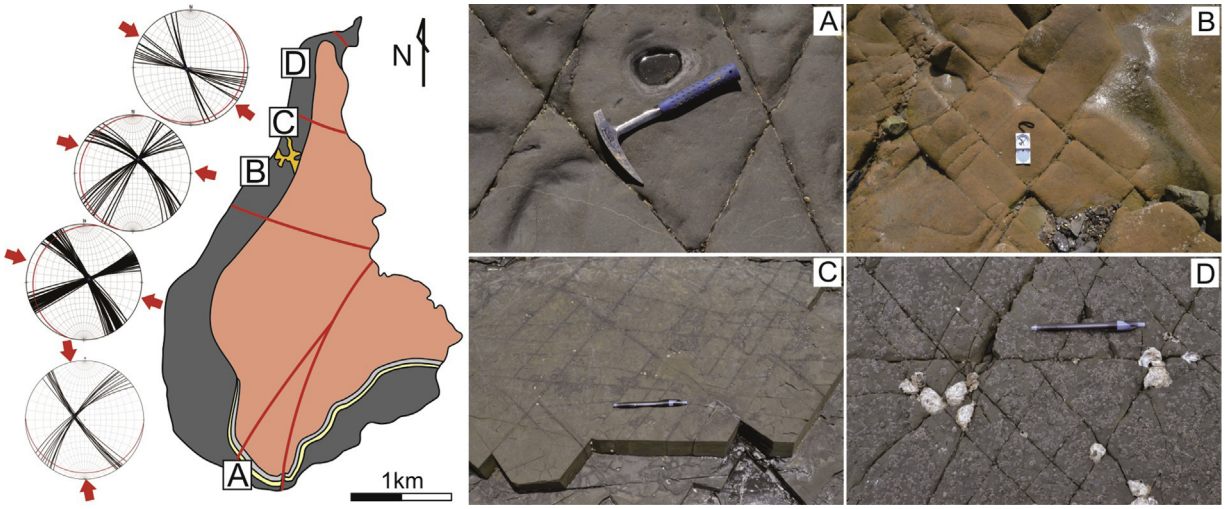

Fig. 9. Stereonet projection of field measurements of conjugated joints from four sections on Lingshan Island, documenting a NW–SE compressional regime to the southeast of the SOB. Measurements of the joint planes are listed in Appendix A3.

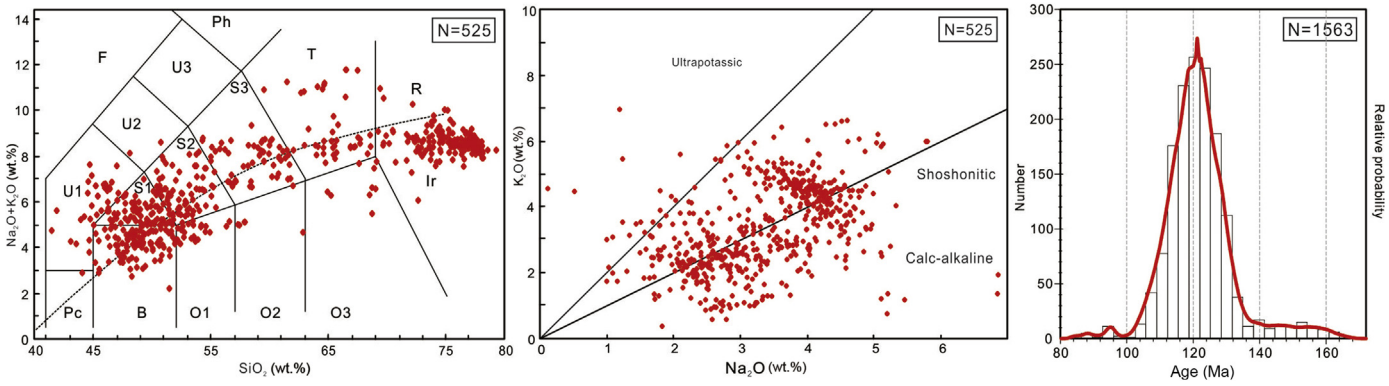

Fig. 10. Geochemical and geochronologic data plots (data and references are compiled in Appendices A4 and A5) for Early Cretaceous igneous bodies from east Shandong. F—Foidite, Ph—Phonolite, U3—Tephri-phonolite, U2—Phonote-phrite, U1—Tephrite/basanite, Pc—Picro/basalt, B—Basalt, T—Trachyte/Trachydacite, S3—Trachy-andesite, S2—Basaltic trachy-andesite, S1—Trachy-basalt, O1—Basaltic andesite, O2—Andesite, O3—Dacite, and R—Rhyolite.

interpretation of southeasterly or southerly transport of material from a YZB source area (Wang et al., 2014).

Age distributions of sandstone samples 612-1 and 428-5 from the JLB resemble each other and include Early Cretaceous, Neoproterozoic, and Paleoproterozoic (1.9–1.8 Ga) ages. These subpopulations indicate a shared source area that accessed widely distributed Early Cretaceous igneous rocks in east Shandong as well as metamorphic units of the SOB and ESC in east Shandong. In contrast to samples from the basin to the southeast of the SOB, JLB samples contained no ~2.0 Ga zircons (Fig. 6). Due to their association with the YZB, clasts from conglomerates of the Laiyang Group in the southwestern part of the JLB (south of the Baichihe-Qingdao-Yantai fault, Fig. 1) have been interpreted as Paleozoic sedimentary cover (Guo and Sun, 1985; Li et al., 2008; Zhou et al., 2012), but YZB basement material has not been reported north of the SOB. The YZB therefore could not contribute source material to this basin since uplift of the SOB ensued from Late Triassic NCB collision, which disrupted YZB access to the JLB source area. According to the detrital zircon age data reported in previous studies, of the three potential source areas, only the YZB contains 2.0 Ga material, an age signature absent from the SOB and ESC. The 2.0 Ga subpopulation has also been detected in age distributions from LSF and BXF samples but not in samples from the JLB. These observations support the interpretation that the SOB did not contribute sediment to the JLB in the Early Cretaceous (Wang et al., 2016a, b).

5.3. Integrated evidence for transtensional tectonics to the northwest of the SOB

Faults, folds, and joints record essential information concerning uplift and tectonic evolution in actively deforming regions like the SOB. This study interpreted tectonic setting using seismic reflection profiles for the JLB along with joint and fold information found in Early Cretaceous sedimentary units south of the SOB. Two N–S seismic reflection profiles (Figs. 1 and 7) of the central JLB were used to interpret basin structure. Both the 50-km and 20-km seismic images include the Cretaceous Laiyang, Qingshan, and Wangshi groups along with underlying Precambrian basement (Fig. 7). A series of south-dipping, low angle normal faults cause limited offset within these units. Sedimentary units pinch out towards the southern margin of the basin, indicating that faults formed in a syn-sedimentary extensional setting following initiation of the JLB. Overall geometry of the JLB therefore indicates a series of detachment faults formed within a crustal-scale extensional setting. Previous studies have interpreted the JLB as a pull-apart structure initiated by sinistral movement along the TLF (Zhu et al., 2005, 2010).

Geochronologic and geochemical analyses of coeval extrusive and intrusive units also indicate Early Cretaceous extensional tectonics in east Shandong (e.g. Zhao and Zheng, 2009, and references therein). As shown by data in Fig. 10 and by previous studies (e.g. Fan et al., 2001), major element total alkali vs. silica diagrams indicate a relatively wide range of basaltic to basalt-andesitic compositions and more tightly constrained rhyolitic compositions. The intermediate samples show relatively scattered compositions. Diagrams of K_2O vs. Na_2O (Fig. 10) indicate a wide range of primarily shoshonitic compositions. The compositional data is typical of bimodal magmatism. Studies have shown that Early Cretaceous magmatism in east Shandong arose from post-collisional lithospheric thinning in an extensional setting (Zheng et al., 2003; Zhu et al., 2012). Mechanisms and associated tectonic evolution remain poorly understood however. The majority of Early Cretaceous igneous events date between 130 Ma and 110 Ma with a remarkable peak at ~120 Ma (Fig. 10). Given sinistral movement along the TLF, we propose that Early Cretaceous igneous events along the SOB led to bimodal intrusive and extrusive volcanism in a transtensional setting.

5.4. Transpressional tectonics southeast of the SOB

Previous studies have recognized an Early Cretaceous transition in the tectonic setting of east China (e.g. Sun et al., 2007; Zhu et al., 2010) but structural and geochronologic evidence for this crustal-scale event is limited. Syn-sedimentary structural observations and detrital zircon age distributions have provided evidence of uplift (e.g. Lu et al., 2011; Wang et al., 2014, 2016b). This study interprets an angular unconformity between folded LSF turbidites and an overlying rhyolite unit found on Lingshan Island (Fig. 8), ~40 km south of the SOB. From lower to upper sections of the LSF, sedimentary facies transition from dark gray marine turbidites consisting of interbedded siltstones and mudstones (e.g. Lu et al., 2011) to grayish brown lacustrine siltstone containing Lecoptera and Yanjiestheria fossils (e.g. Li et al., 2017), then to lacustrine and fluvial sandstones and conglomerates following emplacement of the rhyolite (Wang et al., 2014). In addition to this succession, rapid uplift is also indicated by the ~121 Ma age for the turbidites and a similar age for the overlying rhyolite or tuff (Wang et al., 2014). Gao et al. (2018) interpreted a weighted mean age of ~103 Ma from the six youngest single grains dated from three samples (two grains from each) as the maximum depositional age. This interpretation

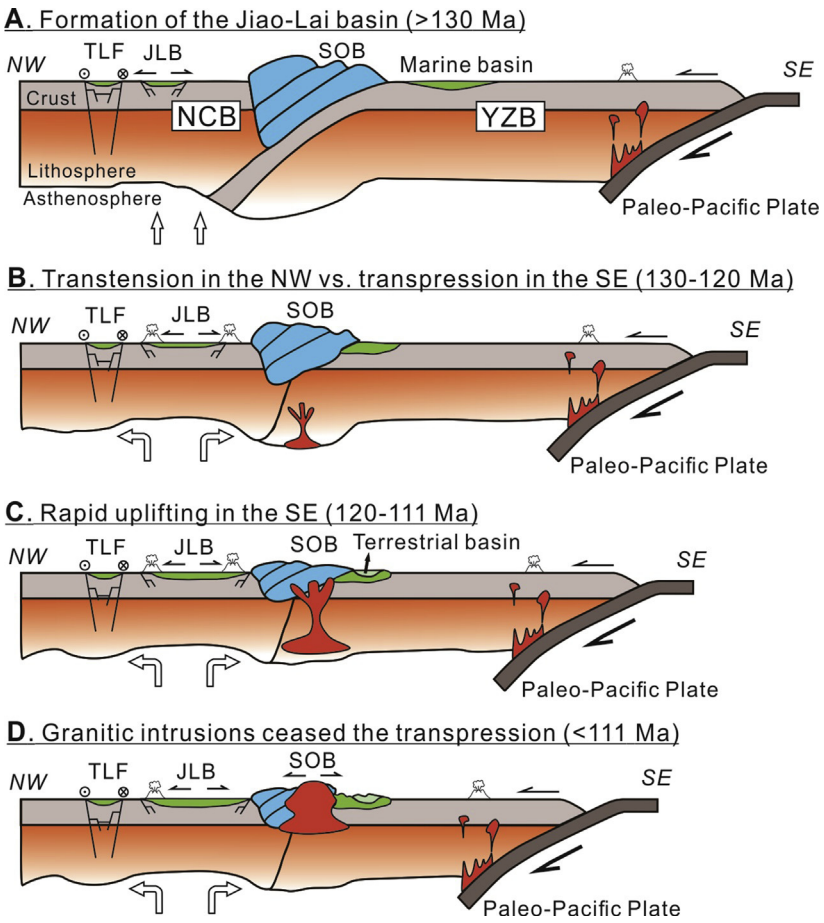

Fig. 11. Early Cretaceous tectonic evolution of the SOB and surrounding areas. TLF —Tan-Lu Fault; JLB — Jiao-Lai Basin; SOB — Sulu Orogenic Belt; NCB — North China Block; YZB — Yangtze Block.

may not have been accurate however since Gao et al. (2018) used the youngest single grain ages instead of the weighted mean age of the youngest subpopulation. We continue to ascribe to the ~122–121 Ma age interpretation by Wang et al. (2016b). We also speculate that initial LSF deposition shifted from marine to lacustrine conditions as the basin began to close due to uplift south of the SOB.

Stereonet projection of conjugated joints observed from different sections of the LSF on Lingshan Island record a NW–SE compressional regime (Fig. 9). Along with the general NW–SE orientation of axial plane directions from syn-sedimentary (Lu et al., 2011) and asymmetrical folds (Fig. 8) in the LSF, structures analyzed indicate a predominantly NW–SE stress field. The evidence of folds (Fig. 8) and conjugated joints (Fig. 9) affecting the LSF but not the overlying rhyolite indicates rapid uplift prior to the eruption of rhyolite in a transpressional tectonic setting, immediately following the sedimentary facies transition. The age at which the joints and the fold formed, as well as the angular unconformity caused by rapid uplift after deposition of the LSF and before emplacement of the rhyolite can be constrained at ~122–121 Ma.

Different phases of syn-sedimentary structures indicate roughly uniform NW–SE compression during deposition of the LSF (e.g. Lu et al., 2011). This evidence accords with the stress field of the folds and conjugate joints in the LSF that formed after deposition. Since the folds and conjugate joints do not appear in overlying rhyolite and fluvial facies, we speculate that NW–SE compression persisted after deposition had ceased (as indicated by the sedimentary facies transition) but predated the eruption of the overlying rhyolite.

5.5. Tectonic evolution of the Jiao-Lai basin

Located to the north of the SOB, the JLB's structures and sedimentary record can be used to reconstruct regional tectonic evolution. Most models of JLB evolution interpret the basin as an extensional feature. For example, Zhang and Dong (2008) and Zhang et al. (2008) posited NW–SE extension from 135 Ma to 120 Ma and subsequent E–W extension from 120 Ma to 100 Ma. Magmatic and metallogenic activity accompanied this latter event. Li et al. (2007) proposed three stages of evolution, which include deposition of the Laiyang Group in an Early Cretaceous extension-related rift basin, deposition of the Qingshan Group with associated Early Cretaceous magmatism, and deposition of the Wangshi Group within a Late Cretaceous dextral, strike-slip-related pull-apart basin. Ni et al. (2013, 2015) proposed rapid Early Cretaceous (ca. 128–123 Ma) exhumation of the Wulian metamorphic core complex in the southern JLB followed by more moderate Late Cretaceous (81–61 Ma) exhumation, consistent with coeval lithospheric extension. Recent studies on the tectonic evolution of east Shandong however have interpreted a tectonic history independent of the SOB. For example, Wang et al. (2016a) suggested a four stage tectonic evolution model for the JLB in the Early Cretaceous. This model includes transpression at >130 Ma, extension from 130 Ma to <110 Ma (based on timing of sinistral strike-slip motion along the TLF), and emplacement of the Laoshan granites along the SOB. Areas of Lingshan Island offer evidence of NW–SE compression at ca. 121 Ma. This timeframe coincides with closure and uplift of the basin hosting LSF and BXF deposition (Wang et al., 2014).

Wang et al. (2016b) recently reinterpreted this tectonic event as transpression occurring from 122–121 Ma to 111 Ma. In recent studies, thermobarometric analysis of Qz-Ab-Or phase diagrams for the granitoids in the northeastern segment of east Shandong indicate rapid crustal exhumation of 130–115 Ma (Dou et al., 2018). This corresponds to the timing of gold mineralization in east Shandong based on zircon geochronology and isotopic analyses (Yang et al., 2018). Both of these studies proposed a shift in tectonic regime from compression to extension at ~121–120 Ma (Dou et al., 2018; Liu et al., 2018; Yang et al., 2018) consistent with the findings of this study. The tectonic setting of the JLB prior to 130 Ma however remains unclear. The tectonic setting and evolution of the JLB thus generally corresponds to that of the basin to the southeast of the SOB, in which the LSF and the BXF formed.

5.6. Tectonic evolution of the SOB during the Early Cretaceous

The SOB's Early Cretaceous history also remains unclear. Based on ophiolites identified along the southwestern margin of the SOB (Fan, 1996, 1998), Wu et al. (2003) proposed the Mesoproterozoic Su-Lu Ocean, a basin formed between the Jiao-Liao craton and the Su-Wan block (incorporating approximate, respective areas of the NCB and YZB). This ocean plate began to subduct southward beneath the Su-Wan block (part of the YZB) in the Triassic, initiating ultrahigh pressure to high pressure metamorphism, and eventually experiencing ocean basin closure by the Jurassic to Early Cretaceous (Wu et al., 2002, 2003). While an abrupt shift in Paleo-Pacific Plate subduction direction and the shift in eastern China's tectonic regime from extension to compression at ca. 125–122 Ma provides an adequate mechanism for explaining cessation of extension related magmatism in southern China, formation of gold deposits in eastern China and sinistral movement along the TLF (Sun et al., 2007), east Shandong itself (which hosts extension-related igneous rocks, gold deposits, and evidence of sinistral movement along the TLF) shows no geological evidence of the shift in plate direction. Evidence instead indicates an extensional tectonic setting. Voluminous extension-related magmatism in the NCB at ca. 130–110 Ma for example (as compiled in Fig. 10) is generally interpreted as resulting from lithospheric thinning (e.g. Menzies et al., 2007; Xu et al., 2009; Yang and Wu, 2009; Lan et al., 2011; Zhang, 2012; Zhu et al., 2012). Structural features associated with the 126–120 Ma gold deposit in east Shandong have been recently re-interpreted as early Mesozoic ductile thrust faults reactivated during Early Cretaceous intracontinental extension (Zhang et al., 2003; Goldfarb and Santosh, 2014). Mylonite micas associated with TLF normal faults gave $^{40}Ar/^{39}Ar$ cooling ages ranging from 129.5 ± 0.8 Ma to 101.8 ± 0.6 Ma, which indicate extension operating in east Shandong during the Early Cretaceous (Zhu et al., 2010).

Evidence provided by multidisciplinary studies focused on the JLB and SOB warrant a reinterpretation of the tectonic setting of the SOB and surrounding areas. While geodynamic mechanisms for intensive late Mesozoic structural, igneous, and sedimentary processes in eastern China remain subject to debate, continuous and generally westward Paleo-Pacific Plate subduction provides a consistent driving force for the tectonic evolution of eastern Asia (Xu, 2001; Menzies et al., 2007; Sun et al., 2007; Xu et al., 2009; Goldfarb and Santosh, 2014). The Late Jurassic to Early Cretaceous shift from subduction of the Izanagi plate to subduction of the Paleo-Pacific Plate beneath eastern China (Zhu et al., 2010) reactivated the TLF causing sinistral faulting and opening of the JLB in the Early Cretaceous. At the same time, the lower part of the thickened NCB crust that predated magmatism (Fan and Menzies, 1992; Griffin et al., 1998; Menzies and Xu, 1998; Davis, 2003; Wang et al., 2006; Xiao and Clemens, 2007) began to melt due to lithospheric thinning (an event whose mechanism remains subject to debate), thus generating magmatic bodies observed throughout the NCB (e.g. Griffin et al., 1998; Menzies and Xu, 1998; Xu, 2001; Xu et al., 2008, 2012; Zhang, 2012). The basin hosting the LSF and BXF had already formed by this time (Fig. 11A). The Paleo-Pacific Plate then changed direction at ca. 125–122 Ma (Sun et al., 2007) thus creating a shift in tectonic setting around the SOB. Southeast of the SOB, sedimentary facies transition in the LSF and a subsequent angular unconformity suggest rapid uplift and closure of the basin at 122–120 Ma caused by transpression (described above). The onset of the change in Paleo-Pacific Plate subduction direction predates uplift of the basin (0–4 m.y.) due to the protracted distance between the SOB and the Paleo-Pacific Plate subduction margin (>1000 km) in the Early Cretaceous. Translation of compressive stress over this distance may have taken a few million years and the intervening sedimentary cover may have also absorbed part of the stress, thereby postponing basin uplift. Concurrently to the northwest of the SOB, the JLB experienced continued extensional stress due to sinistral movement along the TLF (Zhang et al., 2006b; Zhu et al., 2010). Evidence for this extension consists of geochemical and geochronologic data from NCB igneous bodies including those found in east Shandong (described above). Thickening of the SOB lithosphere caused by subduction represents an important mechanism for extensional and transpressional stress indicators observed around the SOB (Fig. 11B). Thickening caused by the Late Triassic NCB-South China Block collision would also dampen or effectively absorb far field effects of stresses related to Paleo-Pacific Plate movement. The basin in which the LSF and BXF deposited experienced compression and uplift while the JLB experienced tension due to lithospheric thinning of the NCB and sinistral movement along the TLF. Later, the depocenter of the basin to the southeast of the SOB transitioned to a terrestrial depositional environment. Extension along the SOB at ca. 111 Ma marked by intrusion of the Late Yanshannian A-type granitoids brought transpressional movement to an end (Zhao et al., 1998a,b; Yan and Shi, 2014; Wang et al., 2016b) (see Fig. 11C). Towards the end of the Early Cretaceous, continued subduction of the Paleo-Pacific Plate led to uplift and erosion of the SOB, which exposed the Yanshannian granites and simultaneously contributed volcaniclastic (Qingshan Group) and terrestrial (Wangshi Group) sedimentary material (Fig. 11D) to the JLB.

6. Conclusions

Detrital zircon U–Pb age distributions from five samples representing basins surrounding the SOB yielded six significant age subpopulations. These included Early Cretaceous (136–110 Ma), Triassic (243–217 Ma), Neoproterozoic (865–568 Ma), Paleoproterozoic (2.0 Ga and 1.9–1.8 Ga), and Archean to Paleoproterozoic (2.5–2.3 Ga) subpopulations used for interpreting provenance and tectonic evolution of the study area. We interpret the Early Cretaceous subpopulation as derived from widely distributed igneous rocks in east Shandong. The Triassic and Neoproterozoic subpopulations likely derived from the SOB. The NCB probably provided observed Archean to Paleoproterozoic subpopulations (2.5–2.3 Ga and 1.9–1.8 Ga), while the YZB likely contributed 2.0 Ga material, a diagnostic subpopulation for differentiating YZB from NCB sedimentary input.

An abrupt shift in the direction of Paleo-Pacific Plate subduction in the Early Cretaceous (~125–122 Ma) together with sinistral movements along the TLF and lithospheric thinning of the NCB provide driving mechanisms for the sequence of events affecting the SOB and surrounding areas. Thickened SOB lithosphere relates

to transpression while reactivated sinistral movement along the TLF and lithospheric thinning of the NCB relate to extension. Thickening of the SOB partially dampened far field effects of the Paleo-Pacific Plate convergence allowing two different tectonic settings to develop around the SOB. These consisted of a trans-tensional setting in the northwest and a transpressional setting in the southeast. Far field effects from the shift in Paleo-Pacific Plate subduction direction predate transpressional evidence of basin rapid uplift at ca. 121–120 Ma. Intrusion of the Late Yanshannian A-type granitoids along the SOB at ca. 111 Ma marked the end of this tectonic framework.

Acknowledgements

This research was supported by the RGC Early Career Scheme (27300114) and General Research Fund grants (17300515) from Hong Kong SAR, China, as well as the Important Scientific and Technological Innovation Project of Shandong Province (2017CXGC1608) from China. We thank Prof. Hong-Bo Lu, Dr. Ying Song, Dr. Gang Lu and Dr. Yunying Zhang for constructive feedback and Prof. Haichun Zhang and Dr. Xiaopeng Dong for their assistance in the field. We also thank editors and two reviewers for their constructive comments.

Appendix A. Supplementary data

Supplementary data to this article can be found online at https://doi.org/10.1016/j.gsf.2019.04.007.

References

Andersen, T., 2002. Correction of common Pb in U-Pb analyses that do not report ^{204}Pb. Chemical Geology 192, 59–79.
Bai, J., Dai, F., 1998. Archean crust of China. In: Ma, X., Bai, J. (Eds.), Precambrian Crustal Evolution of China. Springer, Geological Publishing House, pp. 15–86.
Cai, Y.C., Fan, H.R., Santosh, M., Liu, X., Hu, F.F., Yang, K.F., Lan, T.G., Yang, Y.H., Liu, Y., 2013. Evolution of the lithospheric mantle beneath the southeastern North China Craton: constraints from mafic dikes in the Jiaobei terrain. Gondwana Research 24, 601–621.
Chen, J.F., Xie, Z., Li, H.M., Zhang, X.D., Zhou, T.X., Park, Y.S., Ahn, K.S., Chen, D.G., Zhang, X., 2003. U-Pb zircon ages for a collision-related K-rich complex at Shidao in the Sulu ultrahigh pressure terrane, China. Geochemical Journal 37, 35–46.
Dai, J.S., Lu, K.Z., Song, Q.Y., Chen, S.P., 1995. Kinematic characteristics of Jiaolai basin. Journal of the University of Petroleum 19, 1–6 (in Chinese with English abstract).
Davis, G.A., 2003. The Yanshan belt of North China: tectonics, adakitic magmatism, and crustal evolution. Earth Science Frontiers 10, 373–384.
Deng, J., Liu, X., Wang, Q., Dilek, Y., Liang, Y., 2017. Isotopic characterization and petrogenetic modeling of Early Cretaceous mafic diking-Lithospheric extension in the North China craton, eastern Asia. GSA Bulletin 129, 1379–1407.
Dou, J.Z., Zhang, H.F., Tong, Y., Wang, F., Chen, F.K., Li, S.R., 2018. Application of geothermo-barometers to Mesozoic granitoids in the Jiaodong Peninsula, eastern China: criteria for selecting methods of pressure estimation and implications for crustal exhumation. Journal of Asian Earth Sciences 160, 271–286.
Ernst, W.G., Liou, J.G., 1995. Contrasting plate-tectonic styles of the Qinling-Dabie-Sulu and Franciscan metamorphic belts. Geology 23, 353–356.
Ernst, W.G., Tsujimori, T., Zhang, R.Y., Liou, J.G., 2007. Permo-Triassic collision, subduction-zone metamorphism, and tectonic exhumation along the East Asian continental margin. Annual Review of Earth and Planetary Sciences 35, 73–110.
Fan, J.T., 1996. The Donghai ophiolite of Jinning Episode and the evolution of Su-Jiao orogenic belt, north of Jiangsu. Jiangsu Geology 20, 1–8 (in Chinese with English abstract).
Fan, J.T., 1998. Ophiolite in northern Jiangsu. Journal of Guilin Institute of Technology 18, 136–144 (in Chinese with English abstract).
Fan, W.M., Guo, F., Wang, Y.J., 2001. Post-orogenic bimodal volcanism along the Sulu Orogenic belt in eastern China. Physics and Chemistry of the Earth 26, 733–746.
Fan, W.M., Menzies, M.A., 1992. Destruction of aged lower lithosphere and accretion of asthenosphere mantle beneath eastern China. Geotectonica Mentallogenia 16, 171–180.
Fu, Y.T., Yu, Z.Y., 2010. Metamorphosed marine clastic rocks in Qingdao: tectonic attribute and implication. Chinese Journal of Geology 45, 207–227 (in Chinese with English abstract).
Gao, J., Feng, Q., Zhang, X., Zhou, L., Jiao, Z., Qin, Y., 2018. Zircon U-Pb geochronology of crystal tuff on Lingshan Island and its geological implications for magmatism, stratigraphic age and geological events. Scientific Reports 8, 12718.
Gao, Y., 2015. Origin of A-type Granites in East China: Evidence from Hf-O-Li Isotopes. PhD Thesis. Macquarie University.
Gilder, S.A., Leloup, P.H., Courtillot, V., Chen, Y., Coe, R.S., Zhao, X., Xiao, W., Halim, N., Cogné, J.P., Zhu, R., 1999. Tectonic evolution of the Tancheng-Lujiang (tan-Lu) fault via middle Triassic to early cenozoic paleomagnetic data. Journal of Geophysical Research 104, 15365–15390.
Goldfarb, R.J., Santosh, M., 2014. The dilemma of the Jiaodong gold deposits: are they unique? Geoscience Frontiers 5, 139–153.
Goss, S.C., Wilde, S.A., Wu, F., Yang, J., 2010. The age, isotopic signature and significance of the youngest Mesozoic granitoids in the Jiaodong terrane, Shandong province, north China craton. Lithos 120, 309–326.
Griffin, W.L., Zhang, A.D., O'Reilly, S.Y., Ryan, C.G., 1998. Phanerozoic evolution of the lithosphere beneath the Sino-Korean craton. In: Flower, M.F.J., Chung, S.L., Lo, C.H., Lee, T.Y. (Eds.), Mantle Dynamics and Plate Interactions in East Asia: AGU, vol. 27. Geodynamics Series, Washington, D.C, pp. 107–126.
Guo, F., Fan, W., Li, C., Wang, C.Y., Li, H., Zhao, L., Li, J., 2014. Hf–Nd–O isotopic evidence for melting of recycled sediments beneath the Sulu Orogen, North China. Chemical Geology 381, 243–258.
Guo, F., Fan, W.M., Wang, Y.J., Zhang, M., 2004. Origin of early Cretaceous calc-alkaline lamprophyres from the Sulu orogen in eastern China: implications for enrichment processes beneath continental collisional belt. Lithos 78, 291–305.
Guo, J.H., Chen, F.K., Zhang, X.M., Siebel, W., Zhai, M.G., 2005. Evolution of syn- to post-collisional magmatism from north Sulu UHP belt, eastern China: zircon U-Pb geochronology. Acta Petrologica Sinica 21, 1281–1301 (in Chinese with English abstract).
Guo, Z.Y., Sun, X.Z., 1985. Discovery of oolitic limestone gravels and foraminifer and fusulinid fossils in the upper Jurassic on the southern margin of the Jiao-Lai depression, eastern Shandong and their tectonic significance. Geological Review 31, 179–183 (in Chinese with English abstract).
Hacker, B.R., Ratschbacher, L., Webb, L., Dong, S.W., 1995. What brought them up? Exhumation of the Dabie Shan ultrahigh pressure rocks. Geology 23, 743–746.
Hacker, B.R., Wallis, S.R., McWilliams, M.O., Gans, P.B., 2009. ^{40}Ar/^{39}Ar constraints on the tectonic history and architecture of the ultrahigh-pressure Sulu orogeny. Journal of Metamorphic Geology 27, 827–844.
Hu, F., Fan, H., Yang, J., Wan, Y., Liu, D., Zhai, M., Jin, C., 2004. Mineralizing age of the Rushan lode gold deposit in the Jiaodong deposit in the Jiaodong Peninsula: SHRIMP U-Pb dating on hydrothermal zircon. Chinese Science Bulletin 49, 1629–1636.
Huang, J., Zheng, Y.F., Zhao, Z.F., Wu, Y.B., Zhou, J.B., Liu, X., 2006. Melting of subducted continent: element and isotopic evidence for a genetic relationship between Neoproterozoic and Mesozoic granitoids in the Sulu orogen. Chemical Geology 229, 227–256.
Lan, T.G., Fan, H.R., Santosh, M., Hu, F.F., Yang, K.F., Liu, Y.S., 2011. Geochemistry and Sr-Nd-Pb-Hf isotopes of the Mesozoic Dadian alkaline intrusive complex in the Sulu orogenic belt, eastern China: implications for crust-mantle interaction. Chemical Geology 285, 97–114.
Leech, M.L., Webb, L.E., 2013. Is the HP-UHP Hong'an-Dabie-Sulu orogen a piercing point for offset on the Tan-Lu fault? Journal of Asian Earth Sciences 63, 112–129.
Leech, M.L., Webb, L.E., Yang, T., 2006. Diachronous histories for the Dabie-Sulu orogen from high-temperature geochronology. In: Hacker, B.R., et al. (Eds.), Ultrahigh-pressure Metamorphism: Deep Continental Subduction. Geological Society of America, Special Paper 403, pp. 1–22.
Li, J.L., Zhang, Y.Q., Liu, Z.Q., Ren, F.L., Yuan, J.Y., 2007. Sedimentary-subsidence history and tectonic evolution of the Ljiaolai basin, eastern China. Geology in China 34, 240–250 (in Chinese with English abstract).
Li, S., Zhang, X., Zhao, X., Sun, Z., Zhang, D., Zhang, L., Xu, L., Wei, N., Liu, B., 2017. Discovery of fish and conchostracan fossil in lower cretaceous in Lingshan Island, Qingdao, Shandong. Geological Review 63, 1–6.
Li, S., Zhao, G., 2007. SHRIMP U-Pb zircon geochronology of the Liaoji granitoids: constraints on the evolution of the Paleoproterozoic Jiao-Liao-Ji belt in the eastern block of the north China craton. Precambrian Research 158, 1–16.
Li, S., Zhao, G., Dai, L., Liu, X., Zhou, L., Santosh, M., Suo, Y., 2012. Mesozoic basins in eastern China and their bearing on the deconstruction of the North China Craton. Journal of Asian Earth Sciences 47, 64–79.
Li, S.Y., Meng, Q.R., Li, R.W., Wang, D.X., Chu, S.W., 2008. Characteristics of material components from the lower Cretaceous Laiyang Formation in Jiaolai basin, Shandong province, eastern China and constraints to the provenance. Acta Petrologica Sinica 24, 2395–2406 (in Chinese with English abstract).
Li, X.H., Fan, H.R., Zhang, Y.W., Hu, F.F., Yang, K.F., Liu, X., Cai, Y.C., Zhao, K.D., 2018. Rapid exhumation of the northern Jiaobei terrane, north China craton in the early cretaceous: insights from Al-in-hornblende barometry and U-Pb geochronology. Journal of Asian Earth Sciences 160, 365–379.
Li, X.H., Li, Z., Ge, W., Zhou, H., Li, W., Liu, Y., Michael, T.D., Wingate, T.D., 2003a. Neoproterozoic granitoids in South China: crustal melting above a mantle plume at ca. 825 Ma? Precambrian Research 122, 45–83.
Li, Z.X., 1994. Collision between the North and South China blocks: a crustal detachment model for suturing in the region east of the Tanlu fault. Geology 22, 739–742.
Li, Z.X., Li, X.H., Kinny, P.D., Wang, J., Zhang, S., Zhou, H., 2003b. Geochronology of Neoproterozoic syn-rift magmatism in the Yangtze Craton, South China and correlations with other continents: evidence for a mantle superplume that broke up Rodinia. Precambrian Research 122, 85–109.

Liang, Y., Liu, X., Qin, C., Li, Y., Chen, J., Jiang, J., 2017. Petrogenesis of early cretaceous mafic dikes in southeastern Jiaolai basin, Jiaodong Peninsula, China. International Geology Review 59, 131–150.
Lin, L.H., Wang, P.L., Lo, C.H., Tsai, C.H., Jahn, B., 2005. ^{40}Ar-^{39}Ar thermochronological constraints on the exhumation of ultrahigh-pressure metamorphic rocks in the Sulu terrane of eastern China. International Geology Review 47, 872–886.
Lin, S.F., Li, Z.X., 1995. Collision between the North and South China blocks: a crustal-detachment model for suturing in the region east of the Tanlu fault: comment and reply. Geology 23, 574–576.
Ling, W.L., Duan, R.C., Xie, X.J., Zhang, Y.Q., Zhang, J.B., Cheng, J.P., Liu, X.M., Yang, H.M., 2009. Contrasting geochemistry of the Cretaceous volcanic suites in Shandong province and its implications for the Mesozoic lower crust delamination in the eastern North China craton. Lithos 113, 640–658.
Liou, J.G., Ernst, W.G., Zhang, R.Y., Tsujimori, T., Jahn, B.M., 2009. Ultrahigh-pressure minerals and metamorphic terranes-The view from China. Journal of Asian Earth Sciences 35, 199–231.
Liu, D., Jian, P., Kroner, A., Xu, S., 2006. Dating of prograde metamorphic events deciphered from episodic zircon growth in rocks of the Dabie-Sulu UHP complex, China. Earth and Planetary Science Letters 250, 650–666.
Liu, F., Xu, Z., Liou, J.G., Song, B., 2004. SHRIMP U-Pb ages of ultrahigh-pressure and retrograde metamorphism of gneisses, south-western Sulu terrane, eastern China. Journal of Metamorphic Geology 22, 315–326.
Liu, F., Zhou, Y., Zhang, Z., Yue, B., 2018. Detrital zircon U-Pb geochronology of early Cretaceous sedimentary rocks in Dingzi Bay and Taolin area from the Sulu Orogen: Provenances and tectonic implications. Geological Journal 1–23.
Liu, F.L., Gerdes, A., Robinson, P.T., Xue, H., Ye, J., 2007. Zoned zircon from eclogite lenses in marbles from the Dabie-Sulu UHP terrane, China: a clear record of ultra-deep subduction and fast exhumation. Acta Geologica Sinica-English Edition 81, 204–225.
Liu, F.L., Liou, J.G., 2011. Zircon as the best mineral for P-t-time history of UHP metamorphism: a review on mineral inclusions and U-Pb SHRIMP ages of zircons from the Dabie-Sulu UHP rocks. Journal of Asian Earth Sciences 40, 1–39.
Liu, S., Feng, C., Hu, R., Gao, S., Wang, T., Feng, G., Qi, Y., Coulson, I.M., Lai, S., 2013. Zircon U-Pb age, geochemical, and Sr-Nd-Pb isotopic constraints on the origin of alkaline intrusions in eastern Shandong Province, China. Mineralogy and Petrology 107, 591–608.
Liu, S., Hu, R., Gao, S., Feng, C., Feng, G.Y., Qi, Y.Q., Coulson, I.M., Yang, Y.H., Yang, C.G., Tang, L., 2012. Geochemical and isotopic constraints on the age and origin of mafic dikes from eastern Shandong Province, eastern North China Craton. International Geology Review 54, 1389–1400.
Liu, S., Hu, R., Gao, S., Feng, C., Yu, B., Feng, G., Qi, Y., Wang, T., Coulson, I.M., 2009a. Petrogenesis of Late Mesozoic mafic dykes in the Jiaodong Peninsula, eastern North China Craton and implications for the foundering of lower crust. Lithos 113, 621–639.
Liu, S., Hu, R., Gao, S., Feng, C., Yu, B., Qi, Y., Wang, T., Feng, G., Coulson, I.M., 2009b. Zircon U-Pb age, geochemistry and Sr-Nd-Pb isotopic compositions of adakitic volcanic rocks from Jiaodong, Shandong Province, Eastern China: constraints on petrogenesis and implications. Journal of Asian Earth Sciences 35, 445–458.
Liu, X.M., Gao, S., Diwu, C.R., Ling, W.L., 2008. Precambrian crustal growth of Yangtze craton as revealed by detrital zircon studies. American Journal of Science 308, 421–468.
Long, Q., Hu, R., Yang, Y.Z., Yang, C.Y., Zhou, S., Siebel, W., Chen, F., 2017. Geochemistry of early cretaceous intermediate to mafic dikes in the Jiaodong Peninsula: constraints on mantle source composition beneath eastern China. The Journal of Geology 125, 713–732.
Lu, H.B., Wang, J., Zhang, H.C., 2011. Discovery of the late Mesozoic slump Beds in Lingshan Island, Shandong, and a Pilot research on the regional tectonics. Acta Geologica Sinica 85, 938–946 (in Chinese with English abstract).
Lu, K.Z., Dai, J.S., 1994. The Formation and Evolution of Jiaolai Basin. Petroleum University Press, Beijing, pp. 2–32 (in Chinese).
Ludwig, K.R., 2003. Isoplot V. 3.0: A Geochronological Toolkit for Microsoft Excel. Special Publication. Berkeley Geochronology Center, pp. 1–70. No. 4.
Ma, L., Jiang, S.Y., Hou, M.L., Dai, B.Z., Jiang, Y.H., Yang, T., Zhao, K.D., Pu, W., Zhu, Z.Y., Xu, B., 2014. Geochemistry of early cretaceous calc-alkaline lamprophyres in the Jiaodong Peninsula: implication for lithospheric evolution of the eastern north China craton. Gondwana Research 25, 859–872.
Ma, L., Jiang, S.Y., Hofmann, A.W., Xu, Y.G., Dai, B.Z., Hou, M.L., 2016. Rapid lithospheric thinning of the North China Craton: new evidence from cretaceous mafic dikes in the Jiaodong Peninsula. Chemical Geology 432, 1–15.
Meng, Y., Santosh, M., Li, R., Xu, Y., Hou, F., 2018. Petrogenesis and tectonic implications of early cretaceous volcanic rocks from Lingshan Island in the Sulu orogenic belt. Lithos 312, 244–257.
Menzies, M.A., Xu, Y.G., 1998. Geodynamics of the north China craton, in mantle dynamics and plate interactions in east Asia. In: Flower, M.F.J., Chung, S.L., Lo, C.H., Lee, T.Y. (Eds.), Mantle Dynamics and Plate Interactions in East Asia, vol. 27. AGU, Washington, D.C. Geodynamics Series, pp. 155–165.
Menzies, M.A., Xu, Y.G., Zhang, H.F., Fan, W.M., 2007. Integration of geology, geophysics and geochemistry: a key to understanding the North China Craton. Lithos 96, 1–21.
Ni, J., Liu, J., Tang, X., Yang, H., Xia, Z., Zhang, T., 2015. Early Cretaceous exhumation of the Sulu orogenic belt as a consequence of the eastern Eurasian tectonic extension: insights from the newly discovered Wulian metamorphic core complex, eastern China. Journal of the Geological Society 173, 531–549.
Ni, J.L., Liu, J.L., Tang, X.L., Yang, H.B., Xia, Z.M., Guo, Q.J., 2013. The Wulian metamorphic core complex: a newly discovered metamorphic core complex along the Sulu orogenic belt, eastern China. Journal of Earth Sciences 24, 1–22.
Okay, A.I., Şengör, A.M.C., 1992. Evidence for intracontinental thrust-related exhumation of the ultra-high-pressure rocks in China. Geology 20, 411–414.
Ratschbacher, L., Franz, L., Enkelmann, E., Jonckheere, R., Porschke, A., Hacker, B.R., Dong, S., Zhang, Y., 2006. The Sino-Korean-Yangtze suture, the Huwan detachment, and the Paleozoic-Tertiary exhumation of (ultra) high-pressure rocks along the Tongbai-Xinxian-Dabie Mountains. In: Hacker, B.R., McClelland, W.C., Liou, J.G. (Eds.), Ultrahigh-pressure Metamorphism: Deep Continental Subduction. The Geological Society of America, Special Paper 403, pp. 45–77.
Ratschbacher, L., Hacker, B.R., Webb, L.E., McWilliams, M., Ireland, T., Dong, S., Calvet, A., Chateigner, D., Wenk, H.R., 2000. Exhumation of the ultrahigh-pressure continental crust in east central China: cretaceous and Cenozoic unroofing and the Tan-Lu fault. Journal of Geophysics Research 105, 13303–13338.
Sun, J.W., Fu, Y.T., Lan, C.L., 2014. Trace element geochemical chracteristics of the marine clastic rocks in Qingdao and their sedimentary environments implications. Marine Sciences 38, 75–81 (in Chinese with English abstract).
Sun, W.D., Ding, X., Hu, Y.H., Li, X.H., 2007. The golden transformation of the Cretaceous plate subduction in the west Pacific. Earth and Planetary Science Letters 262, 533–542.
Tam, P.Y., Zhao, G.C., Liu, F.L., Zhou, X.W., Sun, M., Li, S.Z., 2011. Timing of metamorphism in the Paleoproterozoic Jiao-Liao-Ji belt: new SHRIMP U-Pb zircon dating of granulites, gneisses and marbles of the Jiaobei massif in the north China craton. Gondwana Research 19, 150–162.
Tam, P.Y., Zhao, G.C., Zhou, X.W., Guo, J.H., Sun, M., Li, S.Z., Yin, C.Q., Wu, M.L., 2012. Metamorphic P-T path and tectonic implications of medium-pressure pelitic granulites from the Jiaobei massif in the Jiao-Liao-Ji Belt, North China Craton. Precambrian Research 220–221, 177–191.
Tan, J., Wei, J.H., Shi, W.J., Feng, B., Li, Y.J., Fu, L.B., 2013. Origin of dyke swarms by mixing of metasomatized subcontinental lithospheric mantle-derived and lower crustal magmas in the Guocheng fault belt, Jiaodong Peninsula, North China Craton. Geological Journal 48, 516–530.
Tang, H., Zheng, J., Yu, C., Ping, X., Ren, H., 2014. Multistage crust–mantle interactions during the destruction of the north China craton: age and composition of the early cretaceous intrusions in the Jiaodong Peninsula. Lithos 190, 52–70.
Tang, J., Zheng, Y.F., Wu, Y.B., Gong, B., Liu, X.M., 2007. Geochronology and geochemistry of metamorphic rocks in the Jiaobei terrane: constraints on its tectonic affinity in the Sulu orogen. Precambrian Research 152, 48–82.
Tang, J., Zheng, Y.F., Wu, Y.B., Gong, B., Zha, X., Liu, X., 2008. Zircon U-Pb age and geochemical constraints on the tectonic affinity of the Jiaodong terrane in the Sulu orogen, China. Precambrian Research 161, 389–418.
Wallis, S., Tsuboi, M., Suzuki, K., Fanning, M., Jiang, L., Tanaka, T., 2005. Role of partial melting in the evolution of the Sulu (eastern China) ultrahigh-pressure terrane. Geology 33, 129–132.
Wang, J., Chang, S.C., Lu, H.B., Zhang, H.C., 2014. Detrital zircon U-Pb age constraints on Cretaceous sedimentary rocks of Lingshan Island and implications for tectonic evolution of Eastern Shandong, North China. Journal of Asian Earth Sciences 96, 27–45.
Wang, J., Chang, S.C., Lu, H.B., Zhang, H.C., 2015. Geochronology and geochemistry of Early Cretaceous igneous units from the central Sulu orogenic belt: evidence for crustal delamination during a shift in the regional tectonic regime. Journal of Asian Earth Sciences 112, 49–59.
Wang, J., Chang, S.C., Lu, H.B., Zhang, H.C., 2016a. Detrital zircon provenance of the Wangshi and Laiyang groups of the Jiaolai basin: evidence for early cretaceous uplift of the Sulu orogen, eastern China. International Geology Review 58, 719–736.
Wang, J., Chang, S.C., Lin, P.J., Lu, H.B., Zhu, X.Q., Fu, Y.T., Zhang, H.C., 2016b. Evidence of Early Cretaceous transpression in the Sulu orogenic belt, eastern China. Tectonophyics 687, 44–55.
Wang, Q., Wyman, D.A., Xu, J.F., Zhao, Z.H., Jian, P., Xiong, X.L., Bao, Z.W., Li, C.F., Bai, Z.H., 2006. Petrogenesis of Cretaceous adakitic and shoshonitic igneous rocks in the Luzong area, Anhui Province (eastern China): implications for geodynamics and Cu-Au mineralization. Lithos 89, 424–446.
Wiedenbeck, M., Allé, P., Corfu, F., Griffin, W.L., Meier, M., Oberli, F., Quadt, A.V., Roddick, J.C., Spiegel, W., 1995. Three natural zircon standards for U-Th-Pb, Lu-Hf, trace element and REE analyses. Geostandards Newsletter 19, 1–23.
Wu, G.Y., Chen, H.J., Ma, L., Xu, K.D., 2002. Su-Wan block: an independent tectonic unit during period of Tethyan evolution. Journal of Paleogeography 4, 77–87 (in Chinese with English abstract).
Wu, G.Y., Ma, L., Chen, H.J., Xu, K.D., 2003. Tectonic Evolution of the Su-Wan block, Cretaceous of the Su-Lu orogen and orogenesis-coupled basin developing. Geotectonica et Metallogenia 27, 337–353 (in Chinese with English abstract).
Wu, M.L., Zhao, G.C., Sun, M., Bao, Z.A., Tam, P.Y., He, Y.H., 2014a. Tectonic affinity and reworking of the archean Jiaodong terrane in the eastern block of the north China craton: evidence from LA-ICP-MS U-Pb zircon ages. Geological Magazine 151, 365–371.
Wu, M.L., Zhao, G.C., Sun, M., Li, S.Z., Bao, Z.A., Tam, P.Y., Eizenhoefer, P.R., He, Y.H., 2014b. Zircon U-Pb geochronology and Hf isotopes of major lithologies from the Jiaodong terrane: implications for the crustal evolution of the eastern block of the north China craton. Lithos 190–191, 71–84.

Wu, T.Y., Fu, Y.T., 2014. Cretaceous deepwater lacustrine sedimentary sequences from the Northernmost south China block, Qingdao, China. Journal of Earth Sciences 25, 241–251.
Wu, T.Y., Zhao, S.J., Fu, Y.T., 2010. Petrogeochemistrical characteristics and its implicZation for hydrocarbon of the Lower Paleozoic marine siliclastic rocks in Baxiandun, Qingdao. Chinese Journal of Geology 45, 1156–1169 (in Chinese with English abstract).
Wu, Z.P., Li, L., Li, W., Zhou, Y.Q., 2004. Sedimentary pattern of prototype basin in the deposition period of Laiyang formation and the advantageous areas for oil and gas exploration of Jiaolai basin. Geotectonica et Meallogenia 28, 330–337 (in Chinese with English abstract).
Xia, X.P., Sun, M., Zhao, G.C., Li, H.M., Zhou, M.F., 2004. Spot zircon U-Pb isotope analysis by ICP-MS coupled with a frequency quintupled (213nm) Nd-YAG laser system. Geochemical Journal 38, 191–200.
Xiao, L., Clemens, J.D., 2007. Origin of potassic (C-type) adakite magmas: experimental and field constraints. Lithos 95, 399–414.
Xie, S., Wu, Y., Zhang, Z., Qin, Y., Liu, X., Wang, H., Qin, Z., Liu, Q., Yang, S., 2012. U-Pb ages and trace elements of detrital zircons from Early Cretaceous sedimentary rocks in the Jiaolai Basin, north margin of the Sulu UHP terrane: Provenances and tectonic implications. Lithos 154, 346–360.
Xu, W.L., Hergt, J.M., Gao, S., Pei, F.P., Wang, W., Yang, D.B., 2008. Interaction of adakitic melt–peridotite: implications for the high-Mg# signature of Mesozoic adakitic rocks in the eastern North China Craton. Earth and Planetary Science Letters 265, 123–137.
Xu, W.L., Zhou, Q.J., Pei, F.P., Yang, D.B., Gao, S., Li, Q.L., Yang, Y.H., 2012. Destruction of the North China Craton: delamination or thermal/chemical erosion? Mineral chemistry and oxygen isotope insights from websterite xenoliths. Gondwana Research 23, 119–129.
Xu, Y.G., 2001. Thermo-tectonic destruction of the Archean lithospheric keel beneath eastern China: evidence, timing and mechanism. Physics and Chemistry of the Earth Part A 26, 747–757.
Xu, Y.G., Li, H.Y., Pang, C.J., He, B., 2009. On the timing and duration of the destruction of the North China Craton. Chinese Science Bulletin 54, 3379–3396.
Yan, Q., Shi, X., 2014. Geochemistry and petrogenesis of the Cretaceous A-type granites in the Laoshan granitic complex, eastern China. Island Arc 23, 221–235.
Yan, Q., Shi, X., 2016. Geochronology of the Laoshan granitic complex in eastern China and its tectonic implications. Geological Journal 51, 137–148.
Yang, J.H., Chung, S.L., Wilde, S.A., Chu, M.F., Lo, C.H., Song, B., 2005. Petrogenesis of post-orogenic syenites in the Sulu Orogenic Belt, East China: geochronological, geochemical and Nd-Sr isotopic evidence. Chemical Geology 214, 99–125.
Yang, J.H., Chung, S.L., Zhai, M.G., Zhou, X.H., 2004. Geochemical and Sr-Nd-Pb isotopic compositions of mafic dikes from the Jiaodong Peninsula, China: evidence for vein-plus-peridotite melting in the lithospheric mantle. Lithos 73, 145–160.
Yang, J.H., Wu, F.Y., 2009. Triassic magmatism and its relation to decratonization in the eastern North China Craton. Science in China - Series D: Earth Sciences 52, 1319–1330.
Yang, J.S., Wooden, J.L., Wu, C.L., Liu, F.L., Xu, Z.Q., Shi, R.D., Katayama, I., Liou, J.G., Maruyama, S., 2003. SHRIMP U-Pb dating of coesite-bearing zircon from the ultra-high-pressure metamorphic rocks, Sulu terrane, east China. Journal of Metamorphic Geology 21, 551–560.
Yang, K.F., Jiang, P., Fan, H.R., Zuo, Y.B., Yang, Y.H., 2018. Tectonic transition from a compressional to extensional metallogenic environment at ~120 Ma revealed in the Hushan gold deposit, Jiaodong, North China Craton. Journal of Asian Earth Sciences 160, 408–425.
Yang, W.C., 2002. Geophysical profiling across the Sulu ultra-high-pressure metamorphic belt, eastern China. Tectonophysics 354, 277–288.
Yin, A., Nie, S., 1993. An indentation model for the north and south China collision and the development of the Tan-Lu and Honam fault systems, eastern Asia. Tectonics 12, 801–813.
Zhai, M., Guo, J., Liu, W., 2005. Neoarchean to Paleoproterozoic continental evolution and tectonic history of the North China Craton: a review. Journal of Asian Earth Sciences 24, 547–561.
Zhai, M.G., Liu, W.J., 2001. The formation of granulite and its contribution to evolution of the continental crust. Acta Petrologica Sinica 17, 28–38 (in Chinese with English abstract).
Zhai, M.G., Liu, W.J., 2003. Palaeoproterozoic tectonic history of the North China craton: a review. Precambrian Research 122, 183–199.
Zhang, H.C., Lu, H.B., Li, J.G., Wang, J., Chang, S.C., Dong, X.P., Zhang, X., Huang, Z.C., Shu, Y.C., Ren, X.M., 2013. The Lingshandao Formation: a new lithostratigraphic unit of the lower cretaceous in Qingdao, Shandong, China. Journal of Stratigraphy 37, 196–202 (in Chinese with English abstract).
Zhang, H.F., 2012. Destruction of ancient lower crust through magma underplating beneath Jiaodong Peninsula, North China Craton: U-Pb and Hf isotopic evidence from granulite xenoliths. Gondwana Research 21, 281–292.
Zhang, H.F., Zhai, M.G., He, Z.F., Peng, P., Xu, B.L., 2004. Petrogenesis and implications of the sodium-rich granites from the Kunyushan complex, eastern Shandong Province. Acta Petrologica Sinica 20, 369–380 (in Chinese with English abstract).
Zhang, S.B., Zheng, Y.F., Wu, Y.B., Zhao, Z.F., Gao, S., Wu, F.Y., 2006a. Zircon U-Pb age and Hf-O isotope evidence for Paleoproterozoic metamorphic event in South China. Precambrian Research 151, 265–288.
Zhang, X.O., Cawood, P.A., Wilde, S.A., Liu, R.Q., Song, H.L., Li, W., Snee, L.W., 2003. Geology and timing of mineralization at the Cangshang gold deposit, northwestern Jiaodong Peninsula, China. Mineralium Deposita 38, 141–153.
Zhang, Y.Q., Dong, S.W., 2008. Mesozoic tectonic evolution history of the Tan-Lu fault zone, China: advances and new understanding. Geological Bulletin of China 27, 1371–1390 (in Chinese with English abstract).
Zhang, Y.Q., Li, J.L., Liu, Z.Q., Ren, F.L., Yuan, J.Y., 2006b. Detachment system in deep of Jiaolai basin and their regional tectonic significance. Oil & Gas Geology 27, 504–511 (in Chinese with English abstract).
Zhang, Y.Q., Li, J.L., Zhang, T., Dong, S.W., Yuan, J.Y., 2008. Cretaceous to Paleocene tectono-sedimentary evolution of the Jiaolai basin and the contiguous areas of the Shandong Peninsula (north China) and its geodynamic implications. Acta Geologica Sinica 82, 1229–1257 (in Chinese with English abstract).
Zhao, G.C., 2014. Precambrian Evolution of the North China Craton. Elsevier, Oxford, p. 194.
Zhao, G.C., Cawood, P.A., Wilde, S.A., Sun, M., 2002. Review of global 2.1-1.8 Ga orogens: implications for a pre-Rodinia supercontinent. Earth-Science Reviews 59, 125–162.
Zhao, G.C., Cawood, P.A., Wilde, S.A., Sun, M., Lu, L.Z., 2000. Metamorphism of basement rocks in the central zone of the north China craton: implications for Paleoproterozoic tectonic evolution. Precambrian Research 103, 55–88.
Zhao, G.C., Sun, M., Wilde, S.A., Li, S.Z., 2005. Late archean to Paleoproterozoic evolution of the north China craton: key issues revisited. Precambrian Research 136, 177–202.
Zhao, G.T., Wang, D.Z., Cao, Q.C., Yu, L.S., 1998. Thermal evolution and its significance of I-A type granitoid complex: the Laoshan granitoid as an example. Science in China (Series D) 41, 529–536 (in Chinese with English abstract).
Zhao, R., Zhang, R.Y., Liou, J.G., Booth, A.L., Pope, E.C., Chamberlain, C.P., 2007. Petrochemistry, oxygen isotopes and U-Pb SHRIMP geochronology of mafic-ultramafic bodies from the Sulu UHP terrane, China. Journal of Metamorphic Geology 25, 207–224.
Zhao, X., Coe, R.S., 1987. Palaeomagnetic constraints on the collision and rotation of North and South China. Nature 327, 141–144.
Zhao, Z.F., Zheng, Y.F., 2009. Remelting of subducted continental lithosphere: petrogenesis of Mesozoic magmatic rocks in the Dabie-Sulu orogenic belt. Science in China (D) 52, 1295–1318.
Zheng, Y.F., Fu, B., Gong, B., Li, L., 2003. Stable isotope geochemistry of ultrahigh pressure metamorphic rocks from the Dabie-Sulu orogen in China: implications for geodynamics and fluid regime. Earth-Science Reviews 62, 105–161.
Zheng, Y.F., Zhang, S.B., 2007. Formation and evolution of Precambrian continental crust in South China. Chinese Science Bulletin 52, 1–12.
Zheng, Y.F., Gong, B., Zhao, Z.F., Wu, Y.B., Chen, F.K., 2008a. Zircon U-Pb age and O isotope evidence for Neoproterozoic low-18O magmatism during supercontinental rifting in South China: implications for the Snowball Earth event. American Jornal of Science 308, 484–516.
Zheng, Y.F., Wu, R.X., Wu, Y.B., Zhang, S.B., Yuan, H., Wu, F.Y., 2008b. Rift melting of juvenile arc-derived crust: geochemical evidence from Neoproterozoic volcanic and granitic rocks in the Jiangnan orogen, South China. Precambrian Research 163, 351–383.
Zheng, D.R., Chang, S.C., Perrichot, V., Dutta, S., Rudra, A., Mu, L., Keyy, R.S., Li, S., Zhang, Q., Zhang, Q., Wong, J., Wang, J., Wang, J., Zhang, H.C., Wang, B., 2018. A Late Cretaceous amber biota from central Myanmar. Nature Communications 9, 3170.
Zhou, J.B., Wilde, S.A., Liu, F.L., Han, J., 2012. Zircon U-Pb and Lu-Hf isotope study of the neoproterozoic Haizhou group in the Sulu orogen: provenance and tectonic implications. Lithos 136–139, 261–281.
Zhou, J.B., Wilde, S.A., Zhao, G.C., Zhang, X.Z., Zheng, C.Q., Jin, W., Cheng, H., 2008a. SHRIMP U-Pb zircon dating of the Wulian complex: defining the boundary between the north and south China cratons in the Sulu orogenic belt, China. Precambrian Research 162, 559–576.
Zhou, J.B., Wilde, S.A., Zhao, G.C., Zheng, C.Q., Jin, W., Zhang, X.Z., Cheng, H., 2008b. SHRIMP U-Pb zircon dating of the neoproterozoic Penglai group and archean gneisses from the Jiaobei terrane, north China, and their tectonic implications. Precambrian Research 160, 323–340.
Zhou, X.M., Sun, T., Shen, W.Z., Shu, L.S., Niu, Y.L., 2006. Petrogenesis of Mesozoic granitoids and volcanic rocks in South China: a response to tectonic evolution. Episodes 29, 26–33.
Zhou, X., Wei, C., Geng, Y., Zhang, L., 2004. Discovery and implications of the high pressure pelitic granulite from the Jiaobei massif. Chinese Science Bulletin 49, 1942–1948.
Zhu, G., Niu, M., Xie, C., Wang, Y., 2010. Sinistral to normal faulting along the tan-Lu fault zone: evidence for geodynamic switching of the east China continental margin. The Journal of Geology 118, 277–293.
Zhu, G., Wang, Y.S., Liu, G.S., Niu, M.L., Xie, C.L., Li, C.C., 2005. $^{40}Ar/^{39}Ar$ dating of strike-slip motion on the Tan-Lu fault zone, East China. Journal of Structural Geology 27, 1379–1398.
Zhu, R.X., Yang, J.H., Wu, F.Y., 2012. Timing of destruction of the north China craton. Lithos 149, 51–60.